Contents

1 General Information

^{1}H and ^{13}C nuclear magnetic resonance (NMR) spectra were recorded on a Bruker AVIII-500 spectrometer (500 MHz and 125 MHz, respectively) and are reported relative to residual solvent signals. Data for ^{1}H NMR are recorded as follows: chemical shift (δ, ppm), multiplicity (s, singlet; d, doublet; t, triplet; q, quadruplet; m, multiplet), integration, and coupling constant (Hz). Data for ^{13}C NMR are reported in terms of chemical shift (δ, ppm). Chiral High Performance Liquid Chromatography (HPLC) were performed on Shimadzu LC-16A using DAICEL IE or IA column (5 μm, 4.6 mm $\times$ 250 mm). Matrix-Assisted Laser Desorption/Ionization Time of Flight Mass Spectrometry (MALDI-TOF MS) were performed on a Bruker microflex LT-MS with 2,4,6-trihydroxyacetophenone monohydrate (0.05 M in methanol) as matrix.

List of Abbreviations

rt: room temperature
CD: circular dichroism
HPLC: high-performance liquid chromatography
NMR: nuclear magnetic resonance
DEPT: distortionless enhancement by polarization transfer
COSY: correlation spectroscopy
HSQC: heteronuclear single-quantum correlation
HMBC: ^{1}H detected heteronuclear multiple bond correlation
NOESY: nuclear overhauser enhancement spectroscopy

2 Assembly of TR and enantiopure DPEDA: FRP-4 and FRP-5

2.1 Synthetic procedure

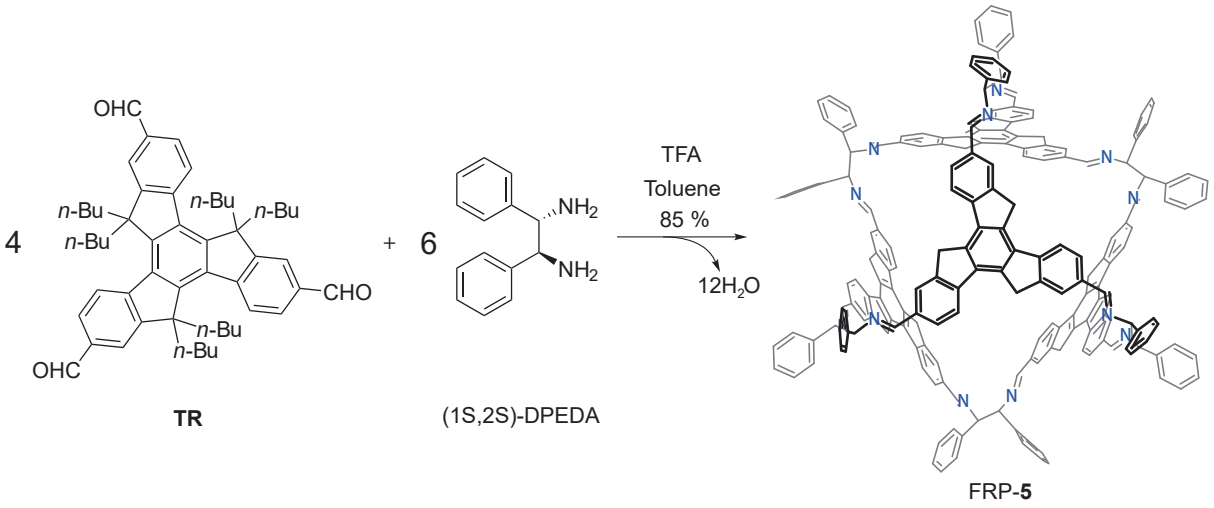

Figure S 1: Synthetic procedure of FRP-**5** using **TR** and (*1S*,*2S*)-diphenylethylenediamine (butyl groups are omitted in stereogram for clarity).

Synthetic procedure:

TR (10.0 mg, 13 µmol) and (*1S*,*2S*)-diphenylethylenediamine (5.01 mg, 23.6 µmol) were mixed in toluene (10 mL, anhydrous) using trifluoroacetic acid (0.1 mg, 1 µmol) as catalyst. The reaction was carried out under nitrogen atmosphere. After 24 hours, the solvents were dehydrated by adding potassium carbonate. The solution were filtered and the filtrate were evaporated under vacuum. The final products were obtained as yellow solids and used for characterization without further purification. synthetic procedure of FRP-**4** was similar to that of FRP-**5**.

2.2 Mass spectrum

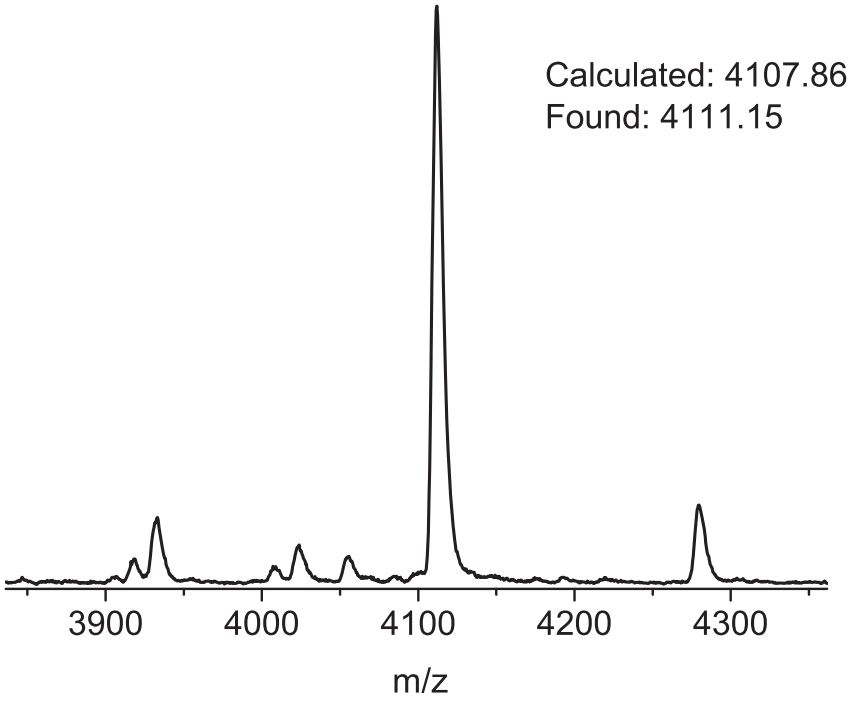

Figure S 2: Low resolution matrix-assisted laser desorption/ionization time of flight mass spectrometry (MALDI-TOF MS) of FRP-**5**.

2.3 Chiral separation spectra of FRP-4 and FRP-5

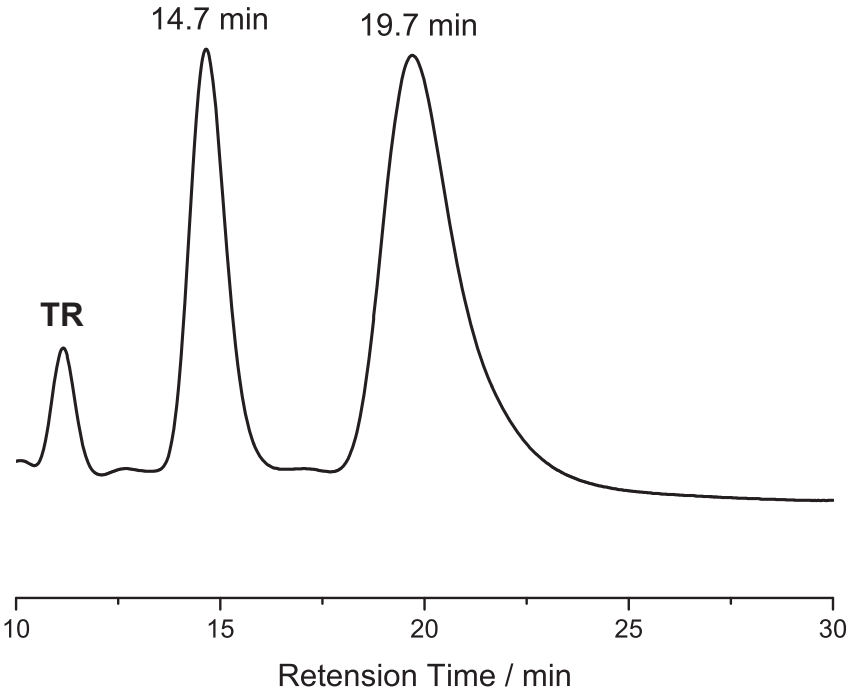

Figure S 3: Chiral separation of polyhedra FRP-**4** assembled by **TR** and (*1R*,*2R*)-DPEDA, the peak eluting at 11.1 minutes was starting material **TR**.

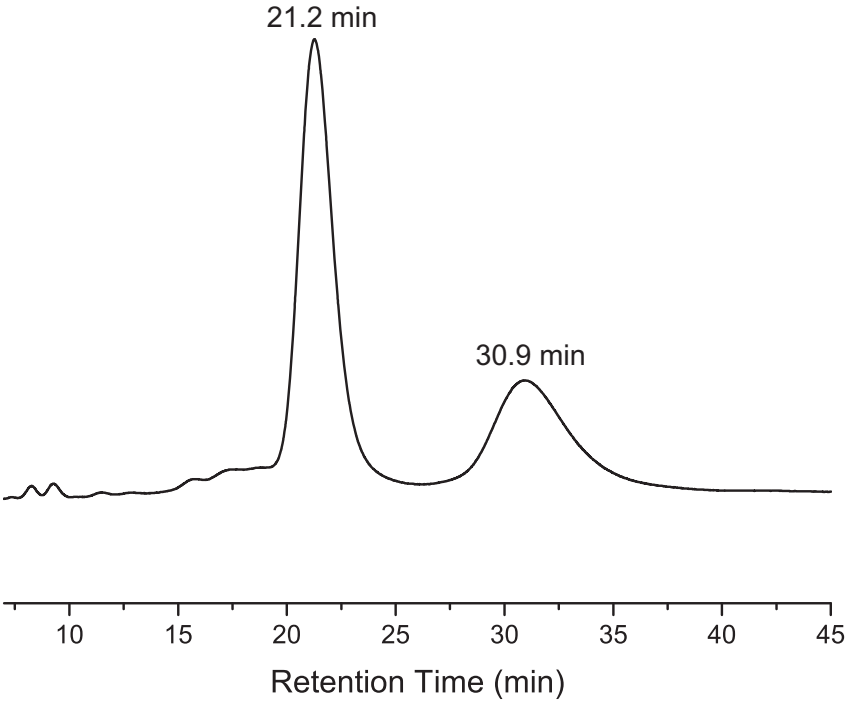

Figure S 4: Chiral separation of FRP-**5** assembled by **TR** and (1S,2S)-DPEDA.

Both FRP-**4** and FRP-**5** were separated by CHIRALPAK IE column using hexane/ethanol (20/80, v/v) as eluent at flow rate of 0.5 ml/min. The spectra were monitored at 325 nm. Two stereoisomers of FRP-**4** eluting at 14.7 minutes and 19.7 minutes (Figure S3) were confirmed by CD and NMR spectra to be (*CAAA*)-**4** and (*AAAA*)-**4**, respectively. FRP-**5** were also found to have two stereoisomers eluting at 21.2 minutes and 30.9 minutes, as shown in Figure S4 and were confirmed to be (*CCCC*)-**5** and (*CCCA*)-**5**, respectively.

2.4 CD spectra of FRP-4 and FRP-5

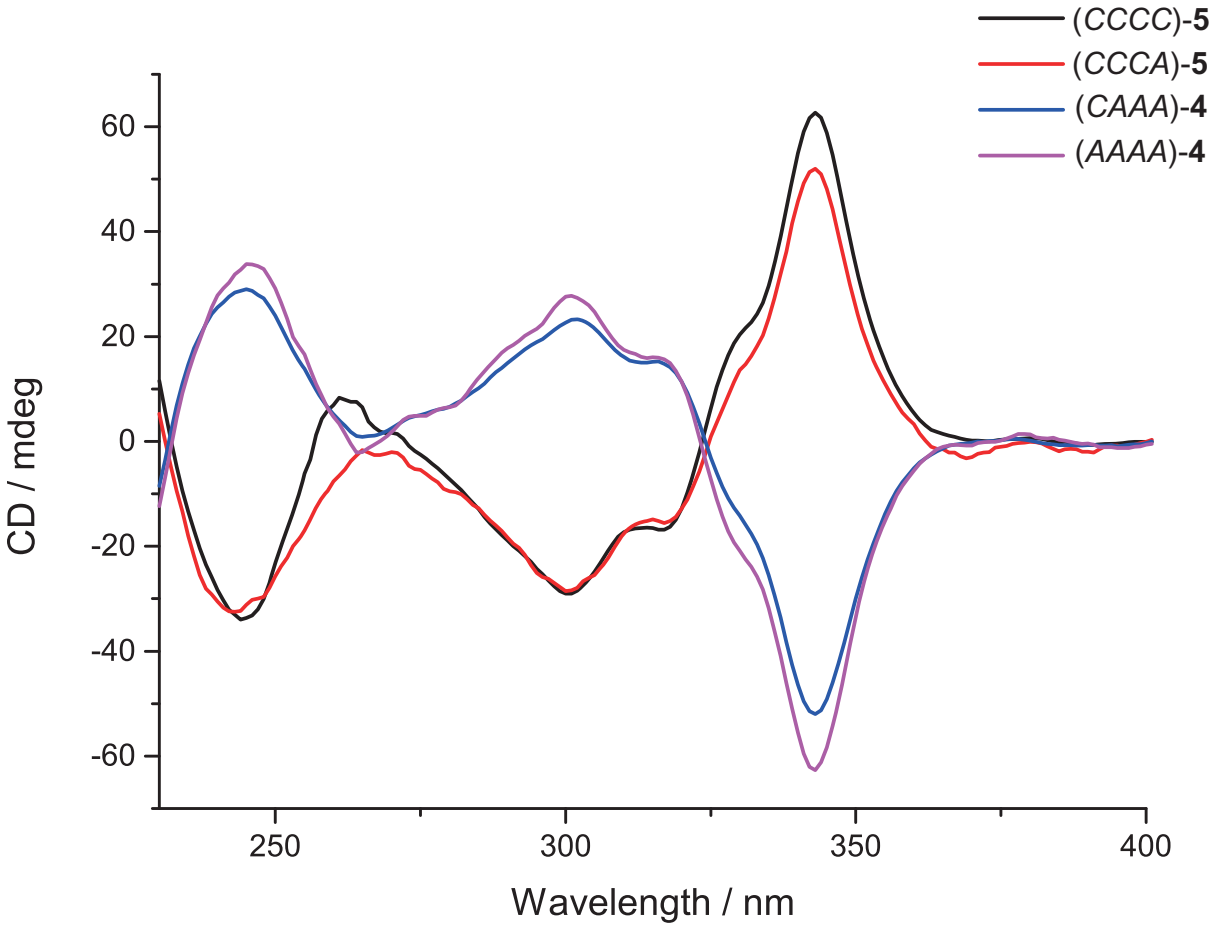

Figure S 5: Experimental CD spectra of four stereoisomers assembled by enantiopure DPEDA, the spectra were measured using hexane/ethanol (20/80, v/v).

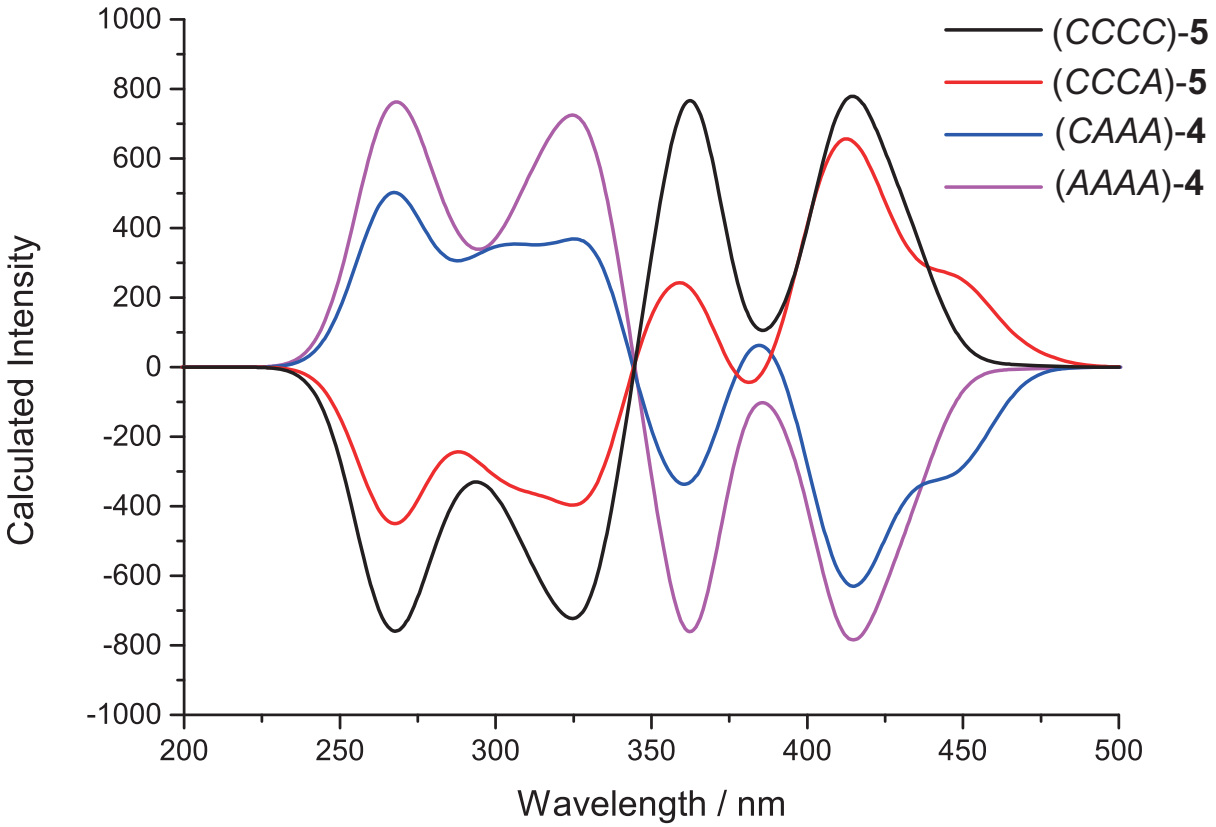

Figure S 6: Calculated CD spectra of four stereoisomers.

Theoretical CD spectra were calculated using ADF software. The geometry of polyhedra were optimized using DFTB3 with 3-ob-3-1 parameter, dispersion correction was D3-BJ. The CD spectra were calculated using TD-DFT+TB method. GGA:BP were applied as the exchange-correlation potential during the SCF procedure. Basis set was TZP (Triple Z, 1 polarization function). Number of lowest excitations to be calculated were set to 2000. Dipole-velocity were also calculated to represent rotatory strength.

2.5 1D and 2D NMR spectra of FRP-5

2.5.1 ^{1}H NMR spectra of crude products

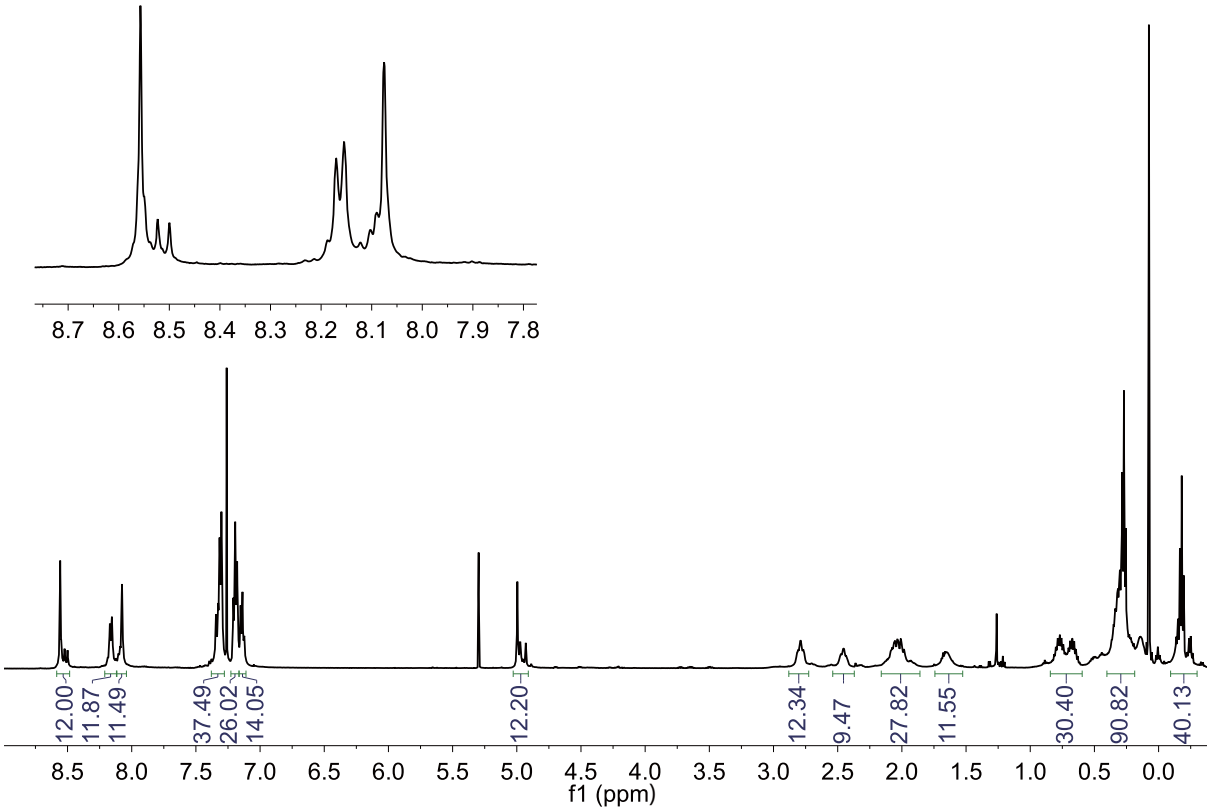

Figure S 7: ^{1}H NMR spectrum of FRP-**5** at room temperature without any purification.

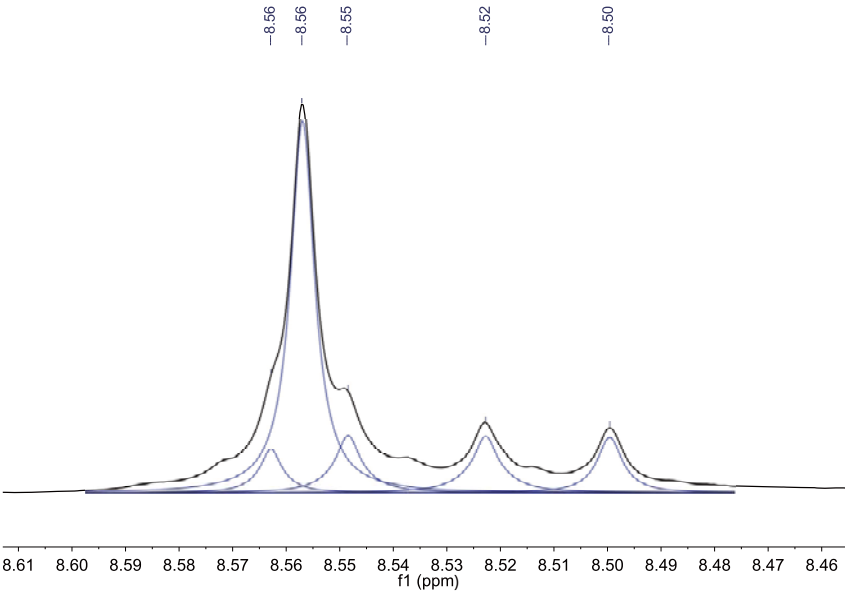

Figure S 8: Fitted lines (blue lines) of experimental NMR peaks (black lines) of imine protons showed one set of singlet and one set of quadruplet, suggesting that two types of stereoisomers exists in FRP-**5**. Thus, the symmetry of two stereoisomers were T and C_3, respectively.

The shape of peaks were fitted using generalized Lorentzian. In NMR spectra of crude products, protons of imine bonds exhibit five peaks, which can be separated into two sets of peaks: one set of singlet and one set of quadruplet, as shown in Figure S8. Hence, FRP-**5** include two types of polyhedra: *T*-symmetric polyhedra (*CCCC*)-**5** exhibiting singlet and C_3-symmetric (*CCCA*)-**5** exhibiting quadruplet. Based on the area of fitted peaks, the ratio of (*CCCC*)-**5** and (*CCCA*)-**5** were determined to be 60% and 40%, respectively. The ratio of (*CCCC*)-**5** and (*CCCA*)-**5** derived from chiral HPLC spectra (65% and 35%).

2.5.2 NMR spectra of (*CCCC*)-5

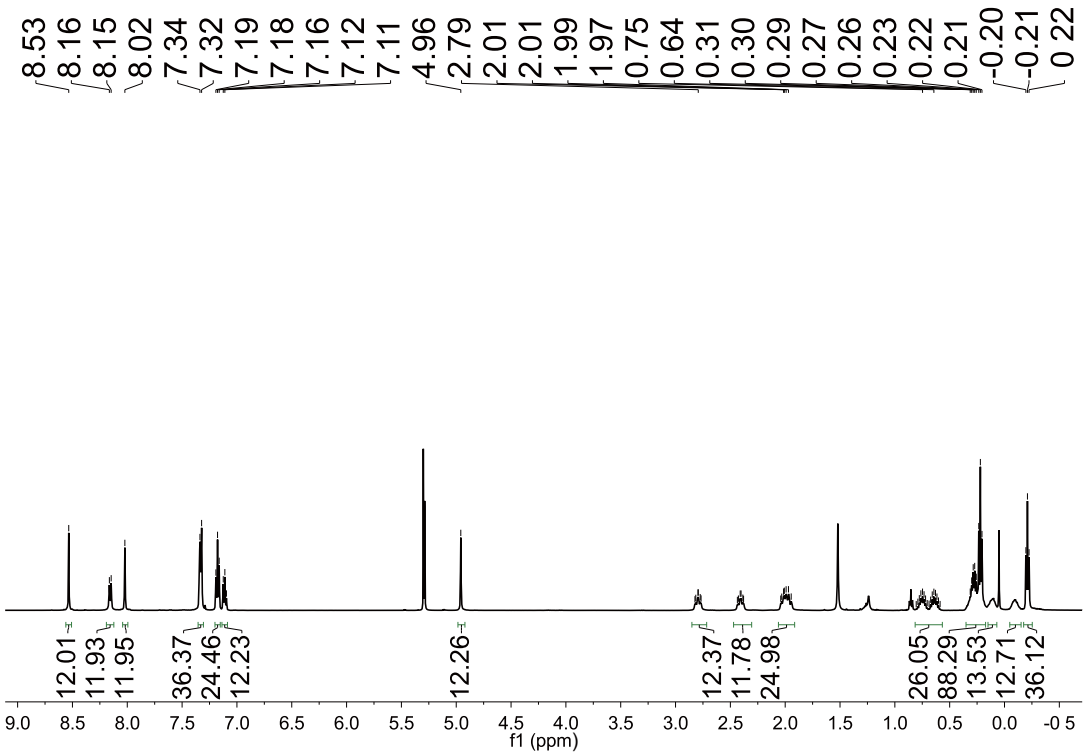

Figure S 9: ^{1}H NMR spectrum of (*CCCC*)-**5**.

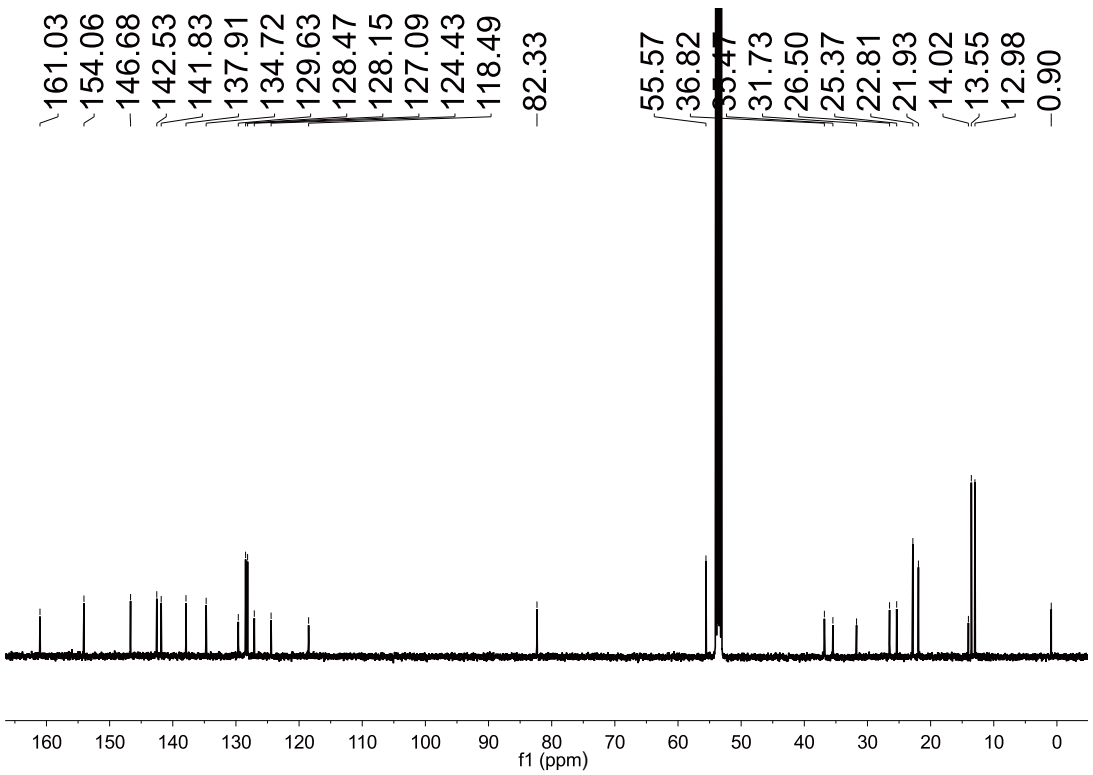

Figure S 10: ^{13}C NMR spectrum of (*CCCC*)-**5**.

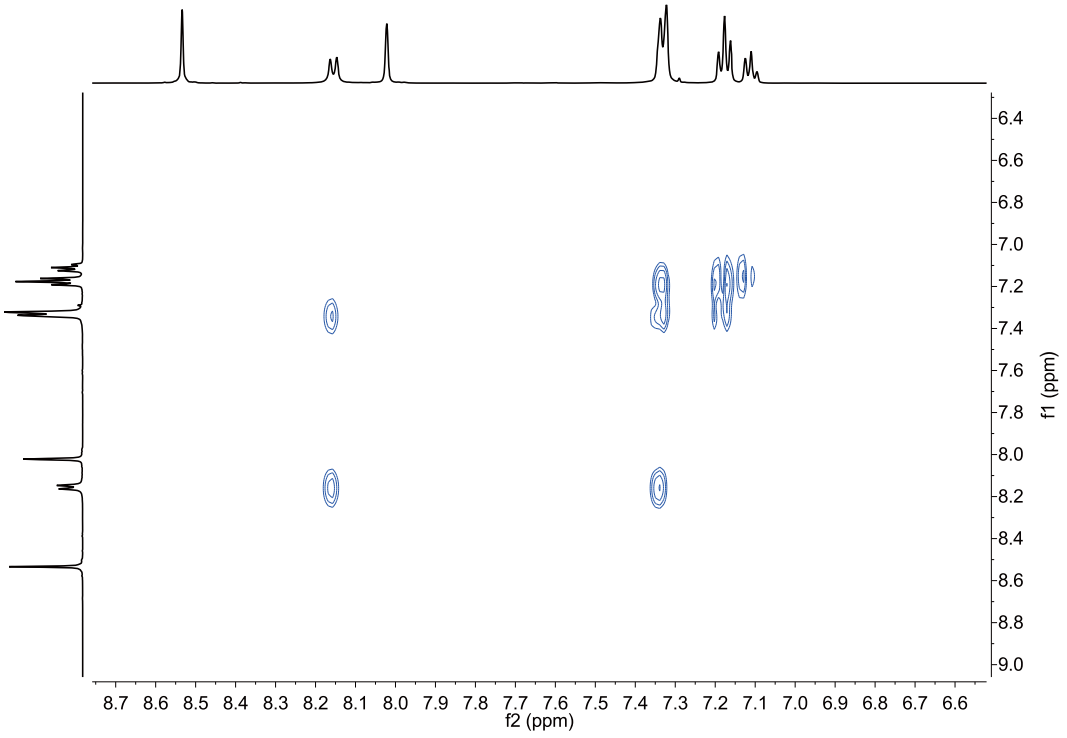

Figure S 11: Partial COSY spectrum of (*CCCC*)-**5**.

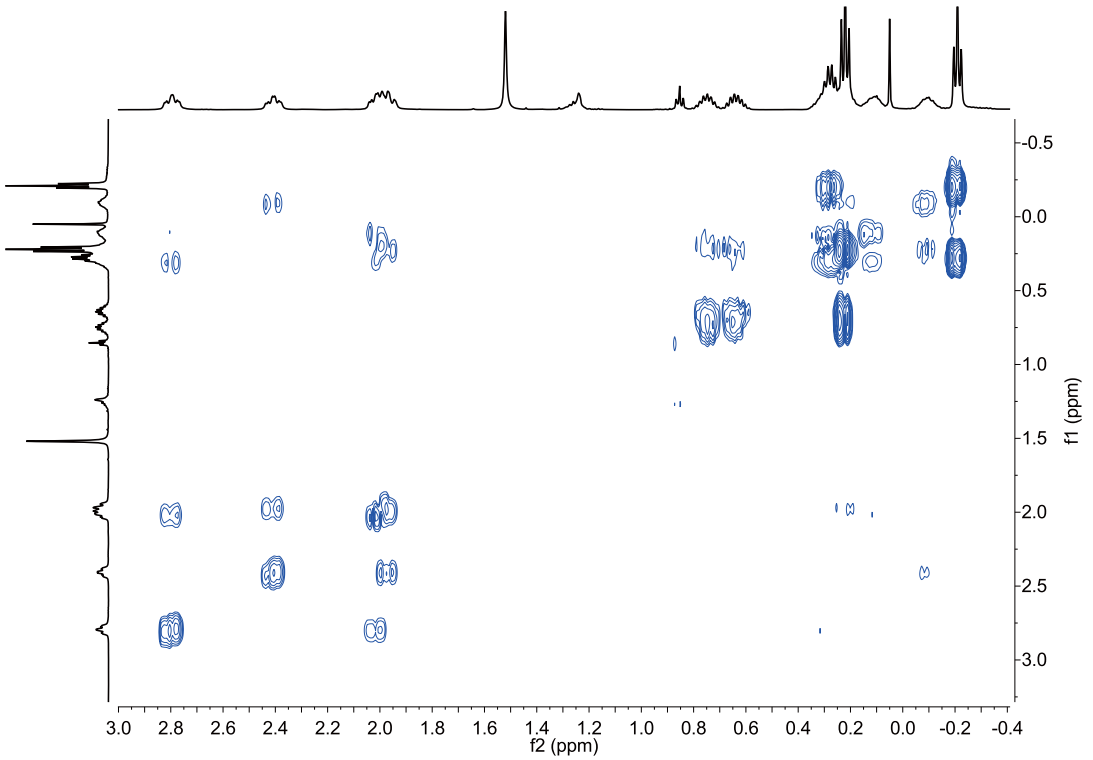

Figure S 12: Partial COSY spectrum of (*CCCC*)-**5**.

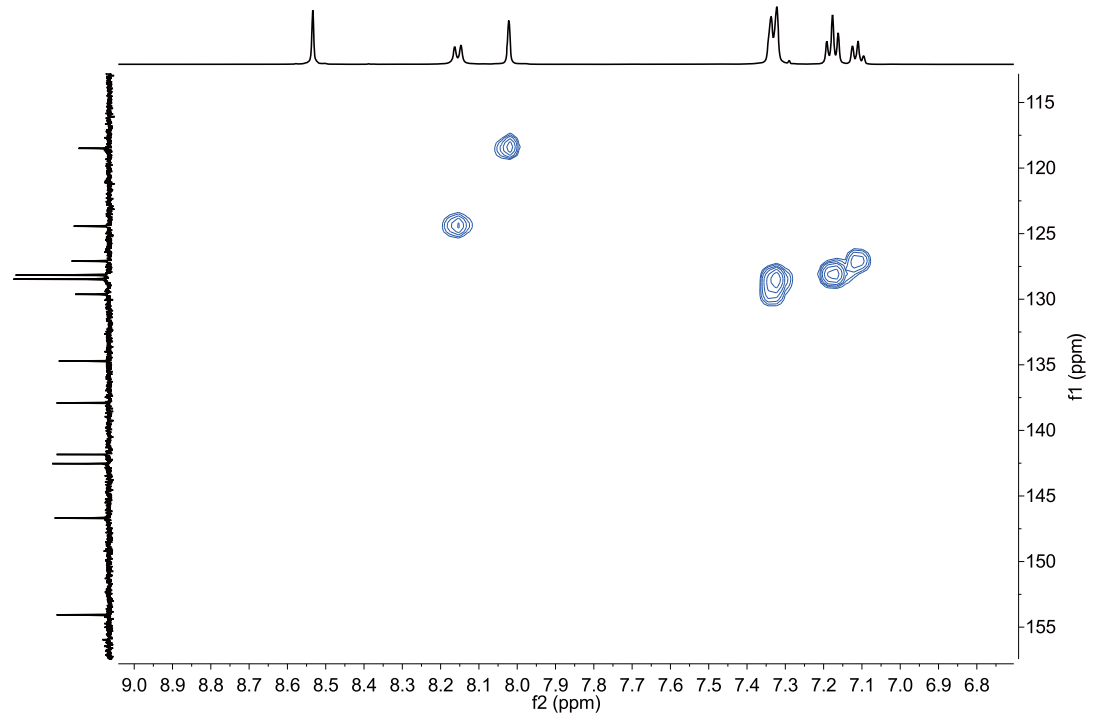

Figure S 13: Partial HSQC spectrum of (*CCCC*)-**5**.

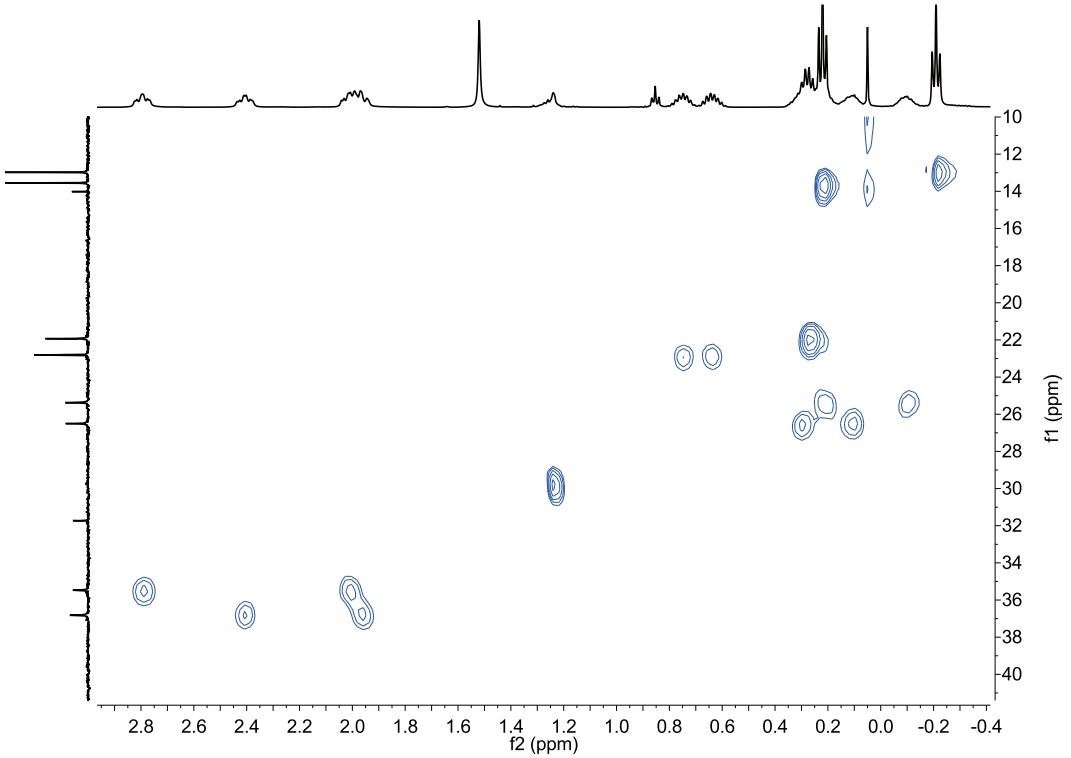

Figure S 14: Partial HSQC spectrum of (*CCCC*)-**5**.

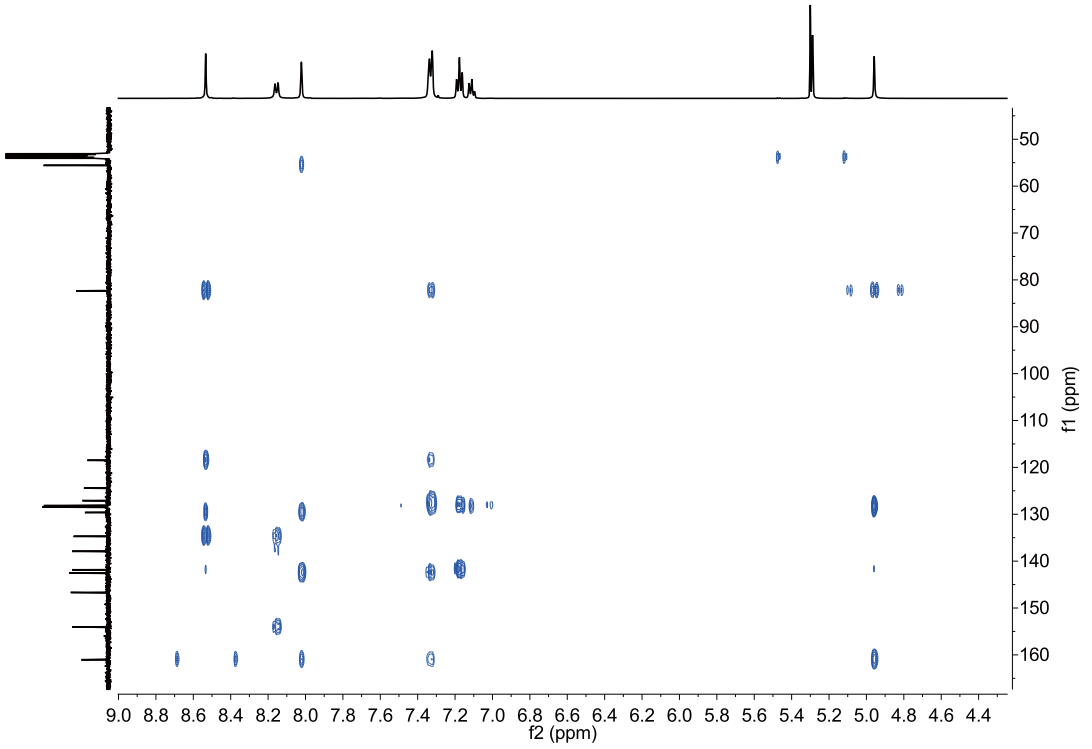

Figure S 15: Partial HMBC spectrum of (*CCCC*)-**5**.

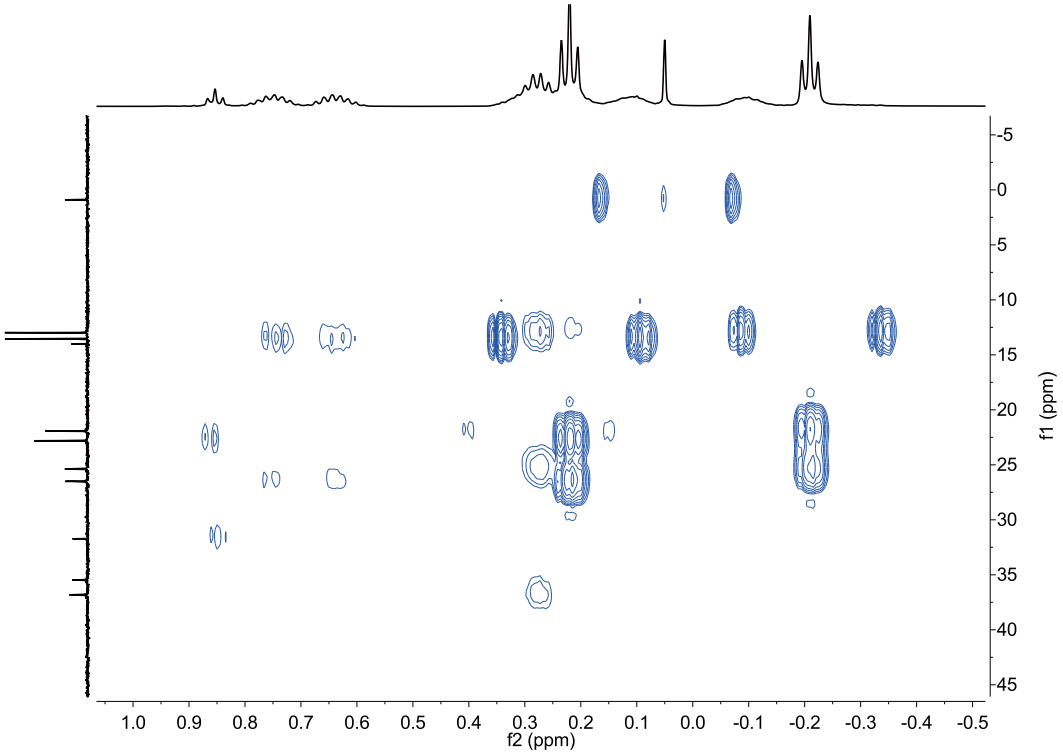

Figure S 16: Partial HMBC spectrum of (*CCCC*)-**5**.

3 Assembly of TR and racemic DPEDA: FRP-6

3.1 Synthetic procedure of FRP-6

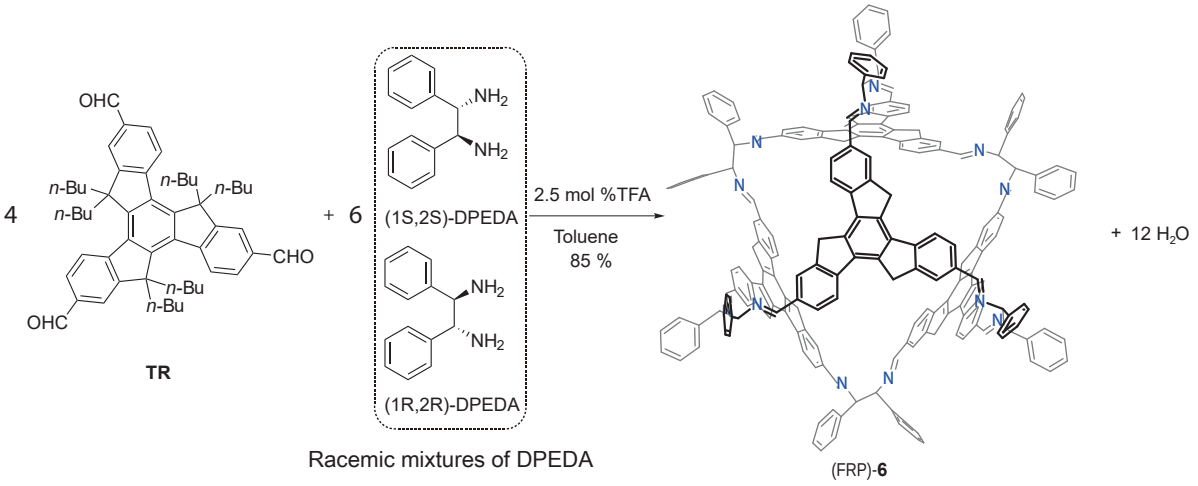

Figure S 17: Synthetic procedure of FRP-**6** assembled by **TR** and racemic diphenylethylenediamine (butyl groups are omitted in stereogram for clarity).

Synthetic procedure

Assembly of **TR** and racemic DPEDA were simliar to that of FRP-**5**. **TR** (13.1 mg, 17 μmol) and racemic DPEDA (7.8 mg, 37.1 μmol) were mixed in toluene (20 mL) with trifluoroacetic acid (0.1 mg, 1 μmol) as catalyst. The products were used without any purification.

3.2 NMR spectra of FRP-6

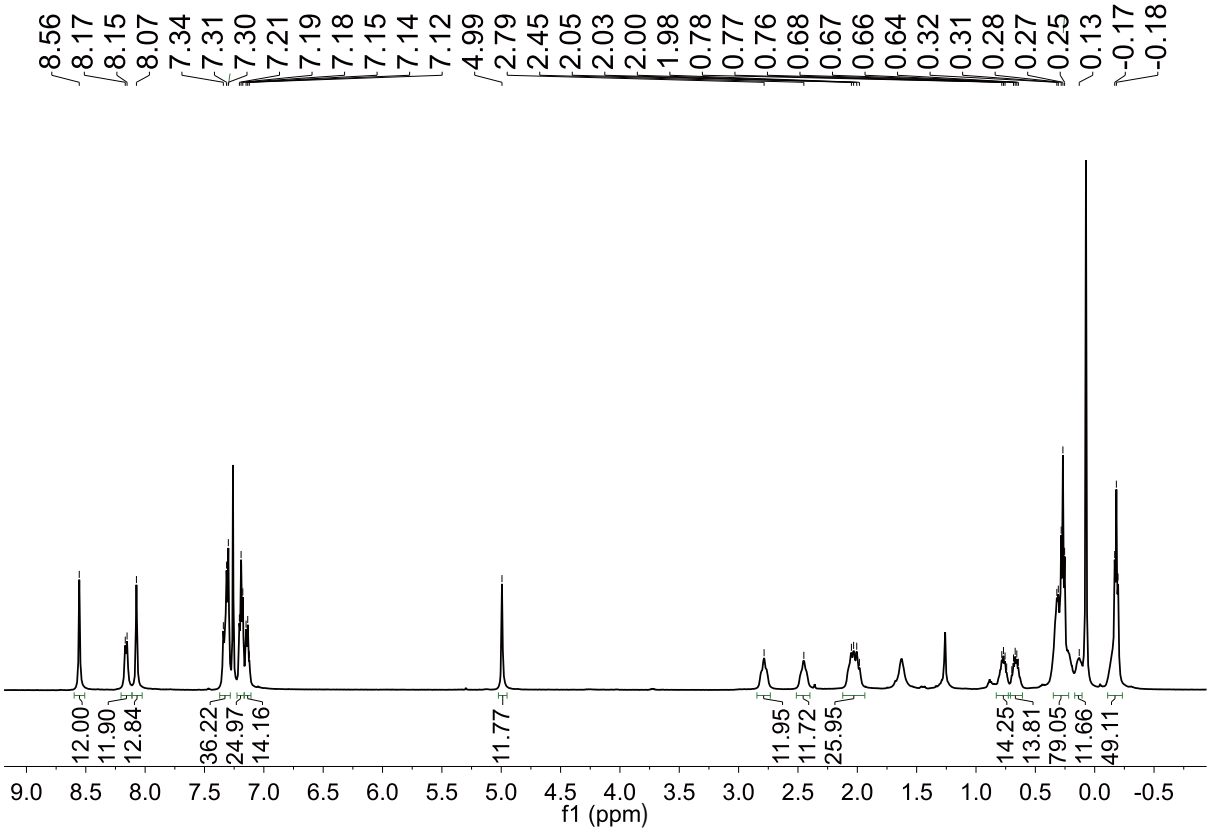

Figure S 18: ^{1}H NMR spectrum of crude products of FRP-**6**, the imine proton (8.56 ppm) exhibit only one set of singlet, suggesting that racemic products contain only *T* symmetric polyhedra.

3.3 Chiral separation of FRP-6

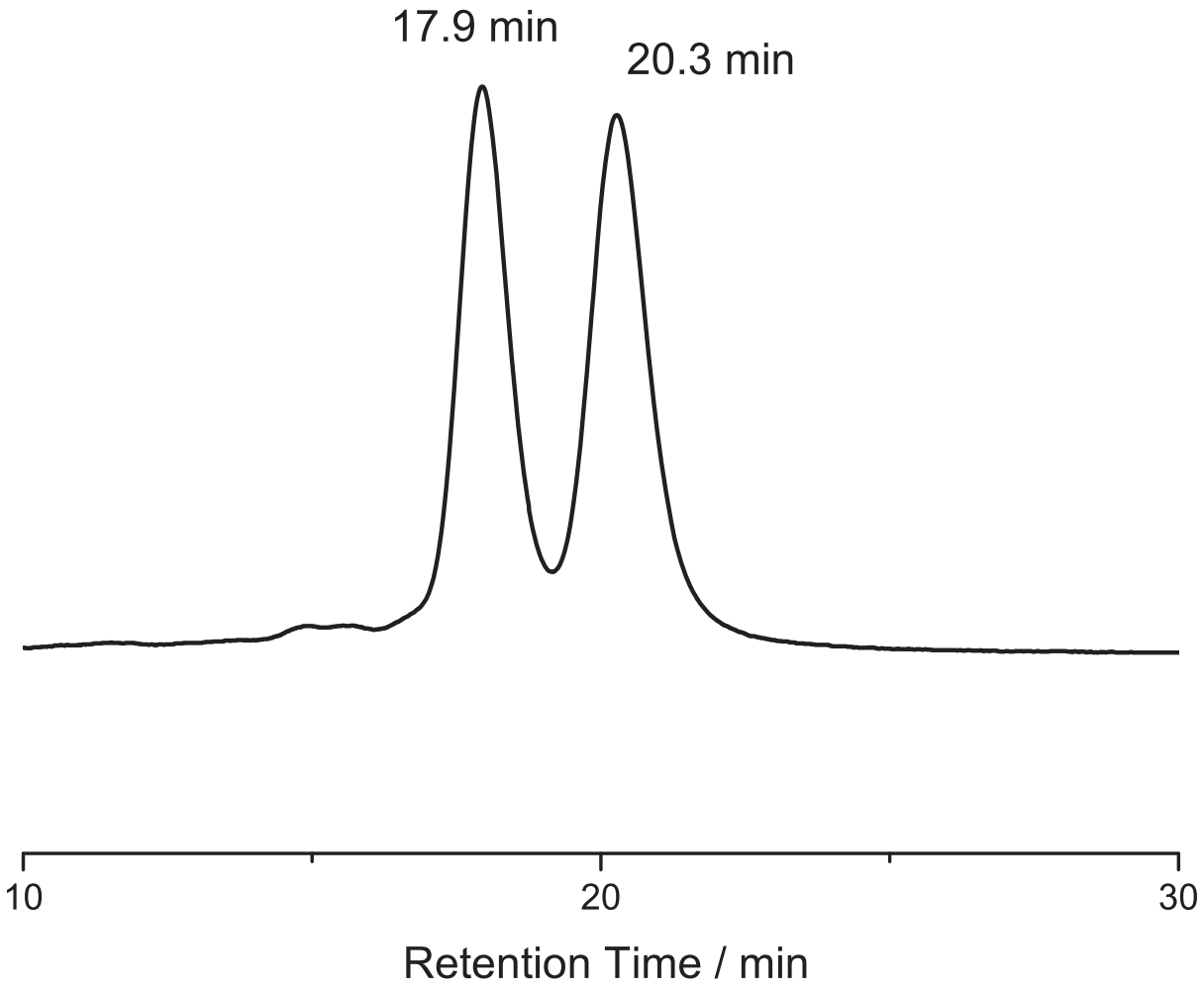

Figure S 19: Chiral separation spectrum of crude products assembled by **TR** and racemic DPEDA without any purification.

Racemic products FRP-**6** were separated by CHIRALPAK IB column from DAICEL using hexane/ethanol (20/80, v/v) as eluent at flow rate of 0.5 ml/min. Two peaks eluting at 17.9 min and 20.3 min were confirmed by CD (Figure S20) to be (*CCCC*)-**5** and (*AAAA*)-**4**, respectively.

3.4 CD spectra of FRP-6

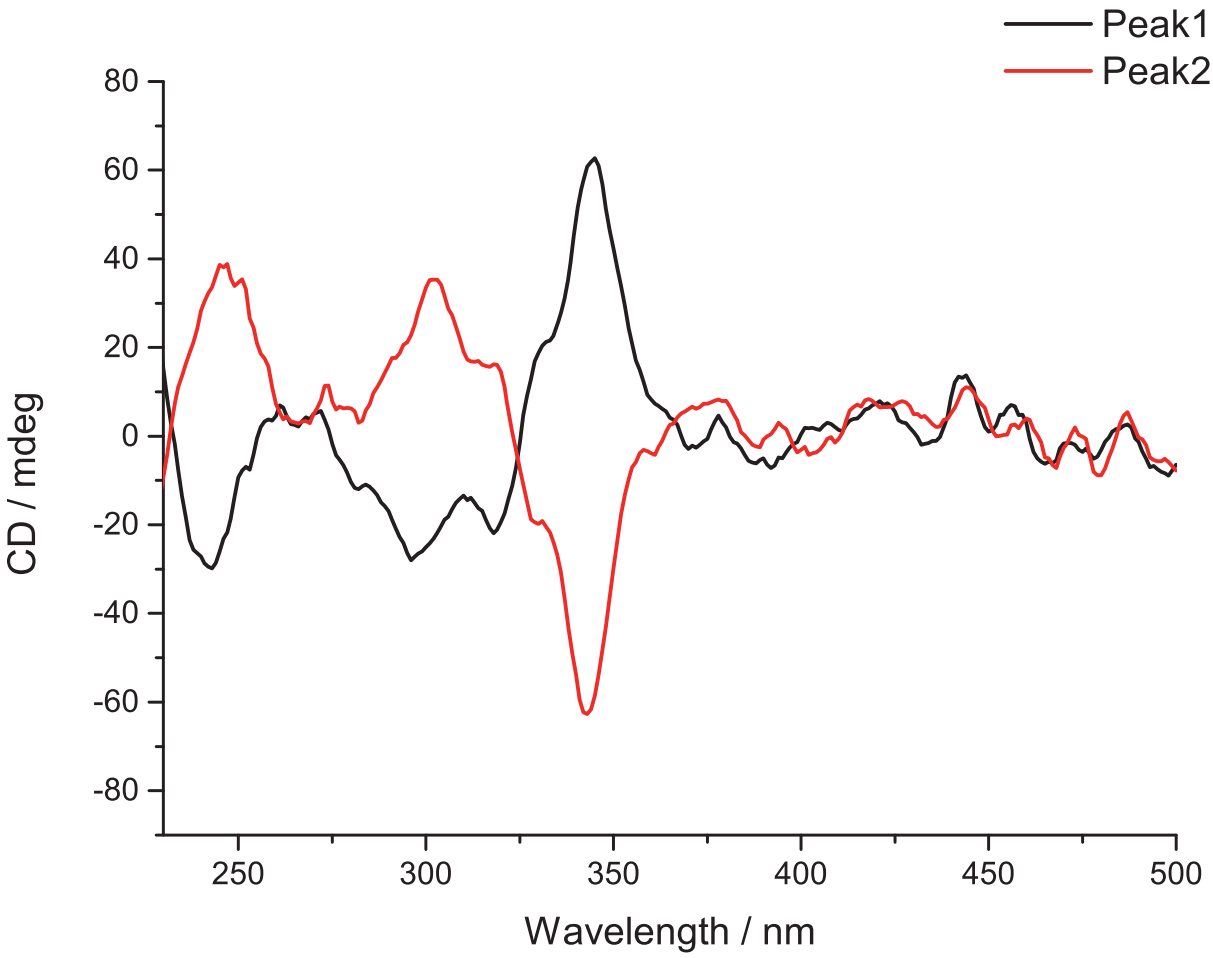

Figure S 20: Experimental CD spectra of the two stereoisomers of FRP-**6** using hexane/ethanol (20/80, v/v).

4 Assembly of TR and racemic CHDA: FRP-7

4.1 Synthetic procedure of FRP-7

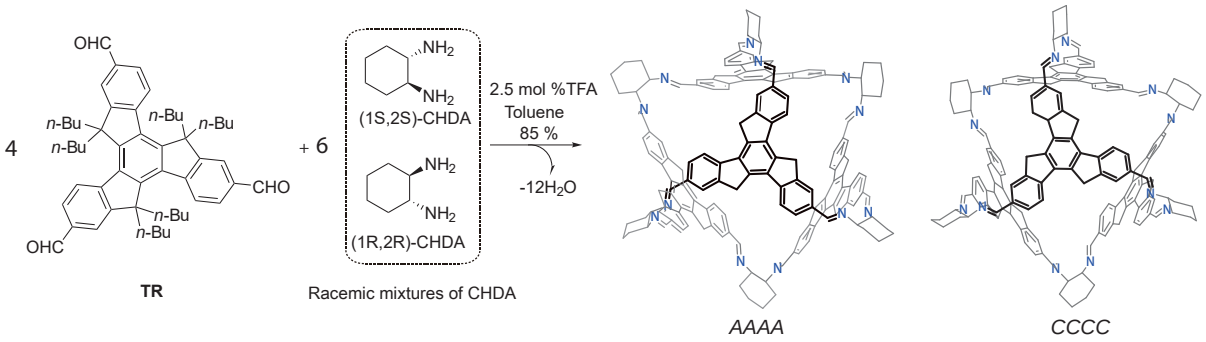

Figure S 21: Synthetic procedure of FRP-**7** assembled by **TR** and racemic CHDA (butyl groups were omitted in sterogram for clarity).

Synthetic procedure:

TR (7 mg, 9.1 μmol) and racemic trans-1,2-diaminocyclohexane (1.6 mg, 13.8 μmol) were mixed in toluene (10 mL) with trifluoroacetic acid (0.07 mg, 0.07 μmol) as catalyst. The reaction was kept at room temperature (or 110 °C). Solvents were evaporated under vacuum and the products were used without any purification.

4.2 NMR spectra of FRP-7

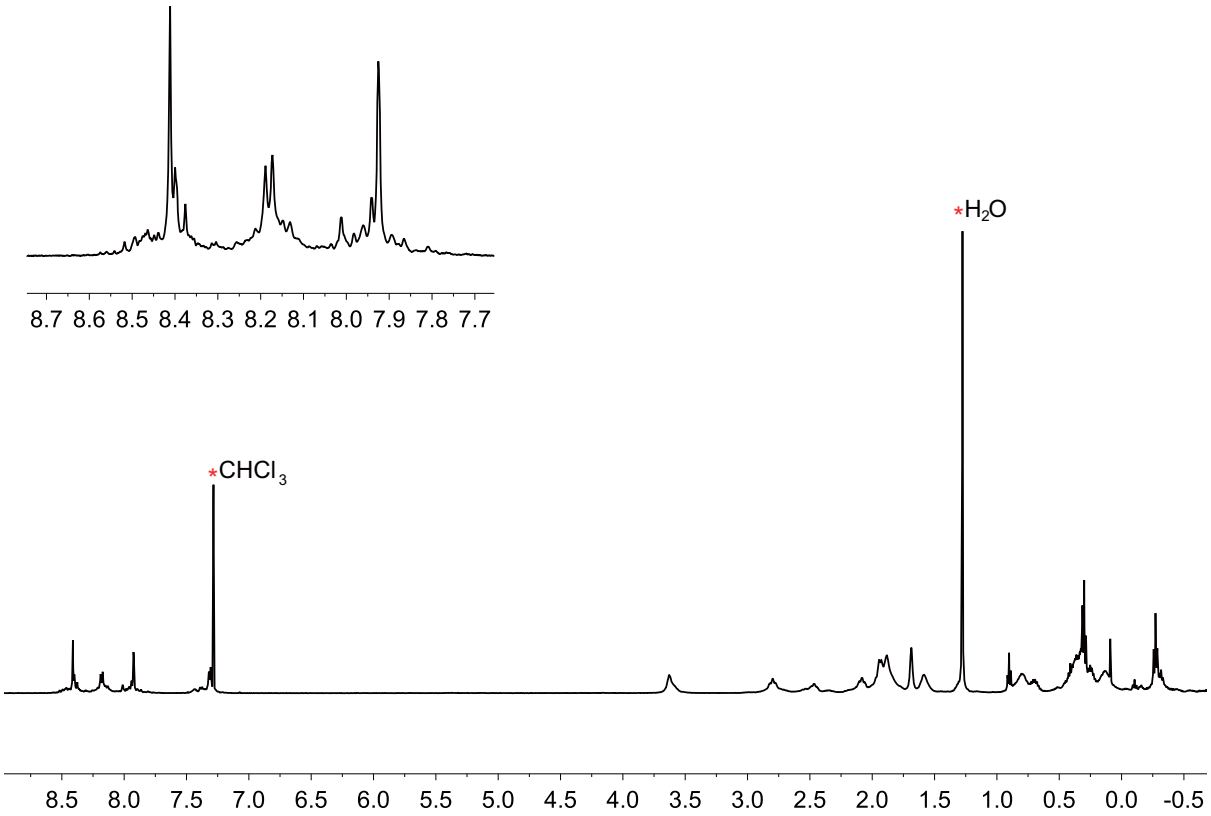

Figure S 22: ^{1}H NMR spectrum of crude products of FRP-**7** at room temperature.

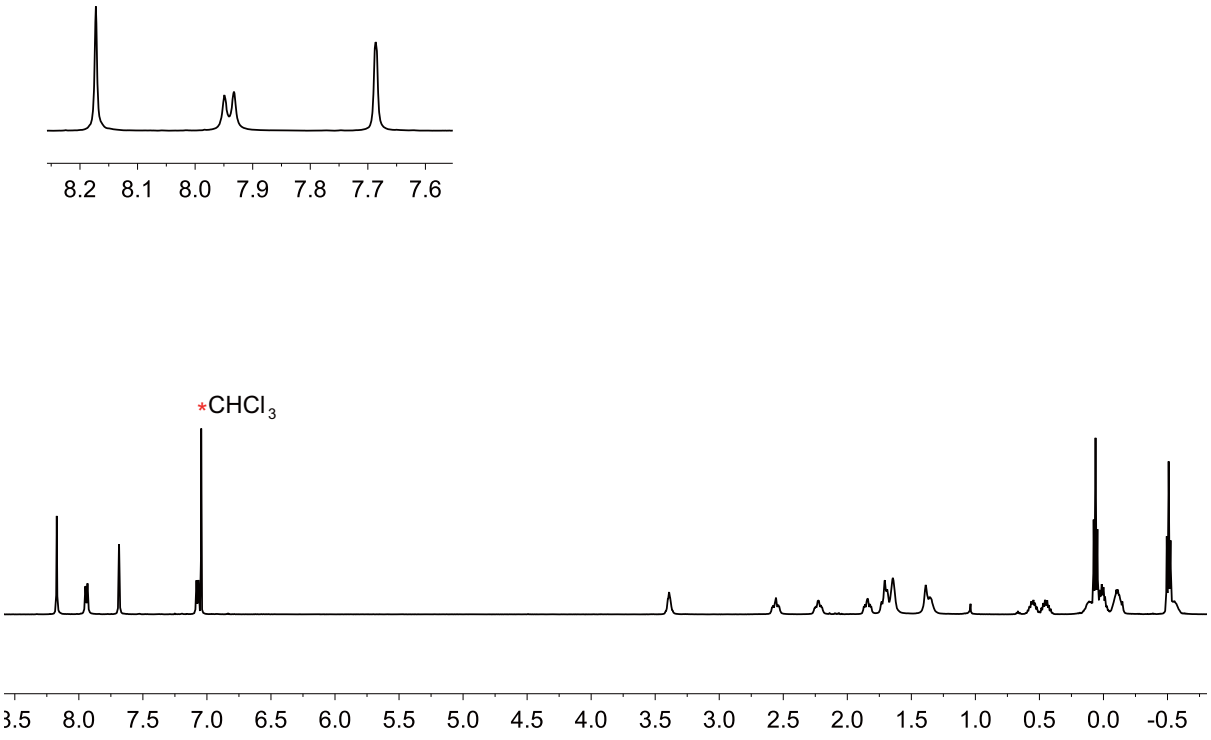

Figure S 23: ^{1}H NMR spectrum of crude products of FRP-**7** assembled at 110 ℃.

4.3 Chiral separation spectra of FRP-7

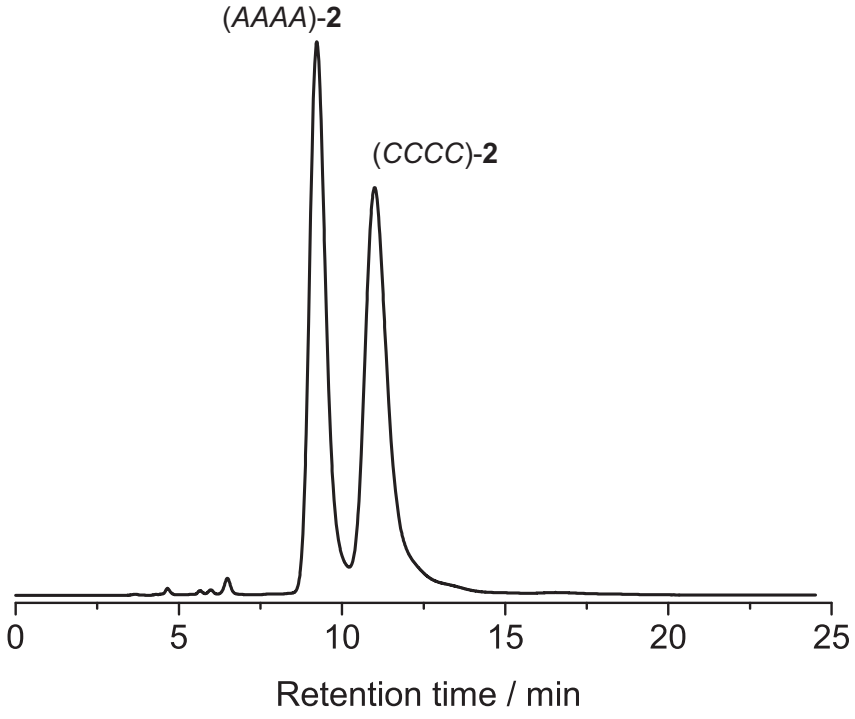

Figure S 24: Chiral separation of racemic products assembled by **TR** and racemic CHDA vertexes.

Racemic polyhedra **2** were separated using CHIRALPAK IE column from DAICEL. The product were separated using hexane/ethanol (80/20, v/v) as mobile phase at flow speed of 1 ml/min. The spectra were monitored at 325 nm. As shown in Figure S24, two peaks existed in FRP-**7** eluting at 9.2 minutes and 11.1 minutes, respectively. Their ^{1}H NMR spectra and CD spectra suggested that the conformation of the first and the second peaks were (*CCCC*)-**5** and (*CCCA*)-**5**, respectively.

4.4 CD spectra of FRP-7

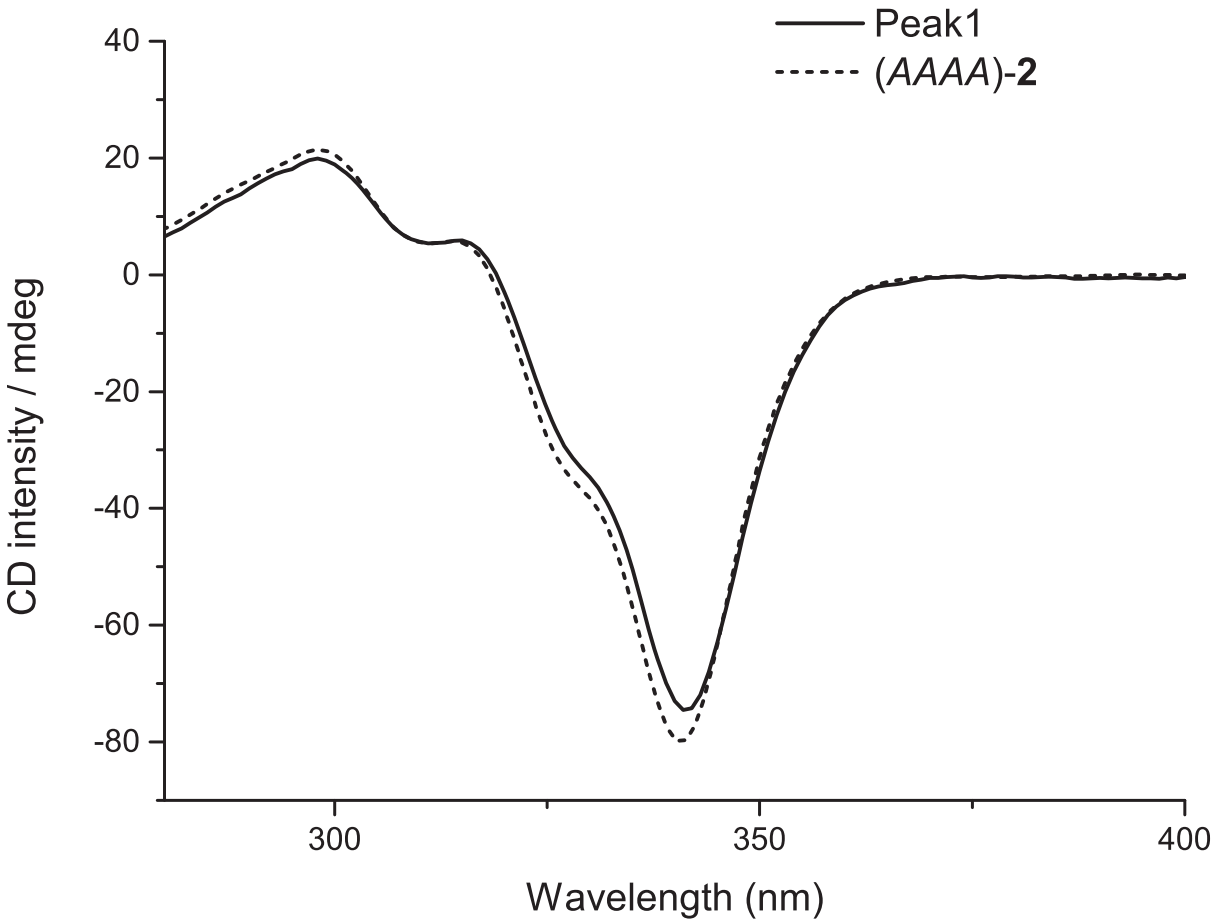

Figure S 25: CD spectra of (*AAAA*)-**2** and first peak of FRP-**7**.

CD spectra of FRP-**7** were measured using hexane/ethanol (20/80, v/v) as solvents and intensity were normalized at maximum absorption of UV-Vis spectra (325 nm).

4.5 Single crystal structures of FRP-7

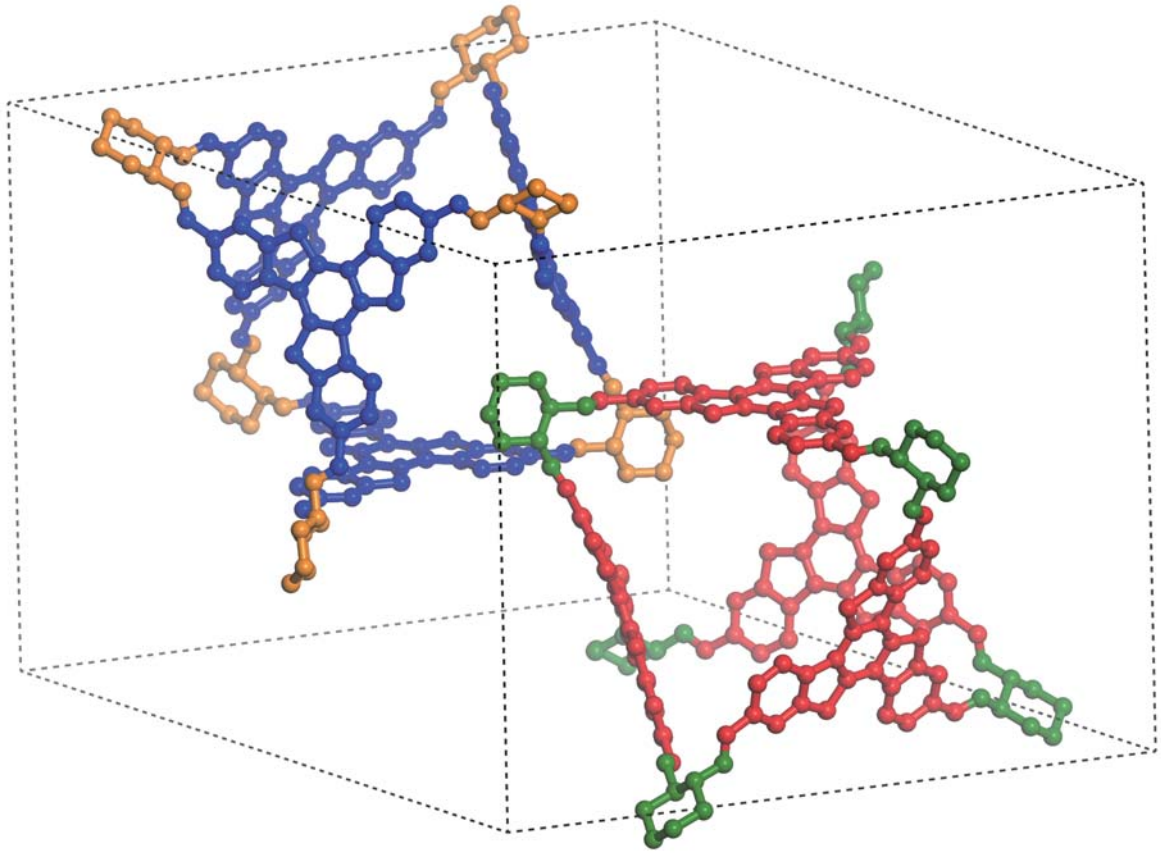

Figure S 26: Single crystal structures of FRP-**7** in unit cell. *CCCC* (blue faces) and *AAAA* (red faces) conformation were found as a pair of enantiomers, chirality of green and orange vertices were R and S, respectively.

5 Possible stereoisomers

The possible stereoisomers of FRP were calculated using Burnside's lemma, which can be used to calculate the number of rotationally distinct colourings of the faces of a polyhedron. For six vertices in a octahedron, the symmetry elements include one *E* (identity operation), three C_2 axes and eight C_3 axes, with 6, 4 and 2 permutation groups, respectively. Thus, the number of permutation of different vertices in a octahedron (N_1) was calculated by the following formula:

$$N_1 = \frac{2^6 + 3 * 2^4 + 8 * 2^2}{1 + 3 + 8} = 12$$

All 12 stereoisomers were demonstrated in Figure S27.

When taking the directionality of faces into consideration, for a octahedron with six R-chiral vertices, the symmetry elements contain one *E*, three C_2 axes and eight C_3 axes, with 4, 2 and 2 permutation groups, respectively. Thus, the number of permutation of different vertices in a octahedron (N_1) was calculated by the following formula:

$$N_2 = \frac{2^4 + 3 * 2^2 + 8 * 2^2}{1 + 3 + 8} = 5$$

All 5 stereoisomers of octahedron **2** were demonstrated in Figure S28.

Similarly, for a octahedron **4** (or its mirror image **3**), the number of possible stereoisomers was calculated to be:

$$N_3 = \frac{2^4 + 1 * 2^2}{1 + 1} = 10$$

All 10 stereoisomers were demonstrated in Figure S29.

For octahedron **7** (or its mirror image **6**), the number of possible stereoisomers was calculated to be:

$$N_4 = \frac{2^4 + 3 * 2^2}{1 + 3} = 7$$

All 7 stereoisomers of 5 were demonstrated in Figure S30.

For octahedron **8** (or its mirror image **5**), the number of possible stereoisomers was calculated to be:

$$N_5 = \frac{2^4}{1} = 16$$

All 16 stereoisomers of octahedron **7** were demonstrated in Figure S31.

For octahedron **9**, the number of possible stereoisomers was calculated to be:

$$N_6 = \frac{2^4}{1} = 16$$

All 16 stereoisomers of octahedron **9** were demonstrated in Figure S32.

For octahedron **10**, the number of possible stereoisomers was calculated to be:

$$N_7 = \frac{2^4}{1} = 16$$

All 16 stereoisomers of octahedron **9** were demonstrated in Figure S33.

For octahedron **11**, the number of possible stereoisomers was calculated to be:

$$N_8 = \frac{2^4 + 2 * 2^2}{1 + 2} = 8$$

All 8 stereoisomers of **11** were demonstrated in Figure S34.

For octahedron **12**, the number of possible stereoisomers was calculated to be:

$$N_9 = \frac{2^4 + 2 * 2^2}{1 + 2} = 8$$

All 8 stereoisomers of **12** were demonstrated in Figure S35.

The total number of possible stereoisomers was:

$$N_{total} = 2*N_2 + 2*N_3 + 2*N_4 + 2*N_5 + N_6 + N_7 + N_8 = 2*5 + 2*10 + 2*7 + 2*16 + 16 + 16 + 8 + 8 = 124$$

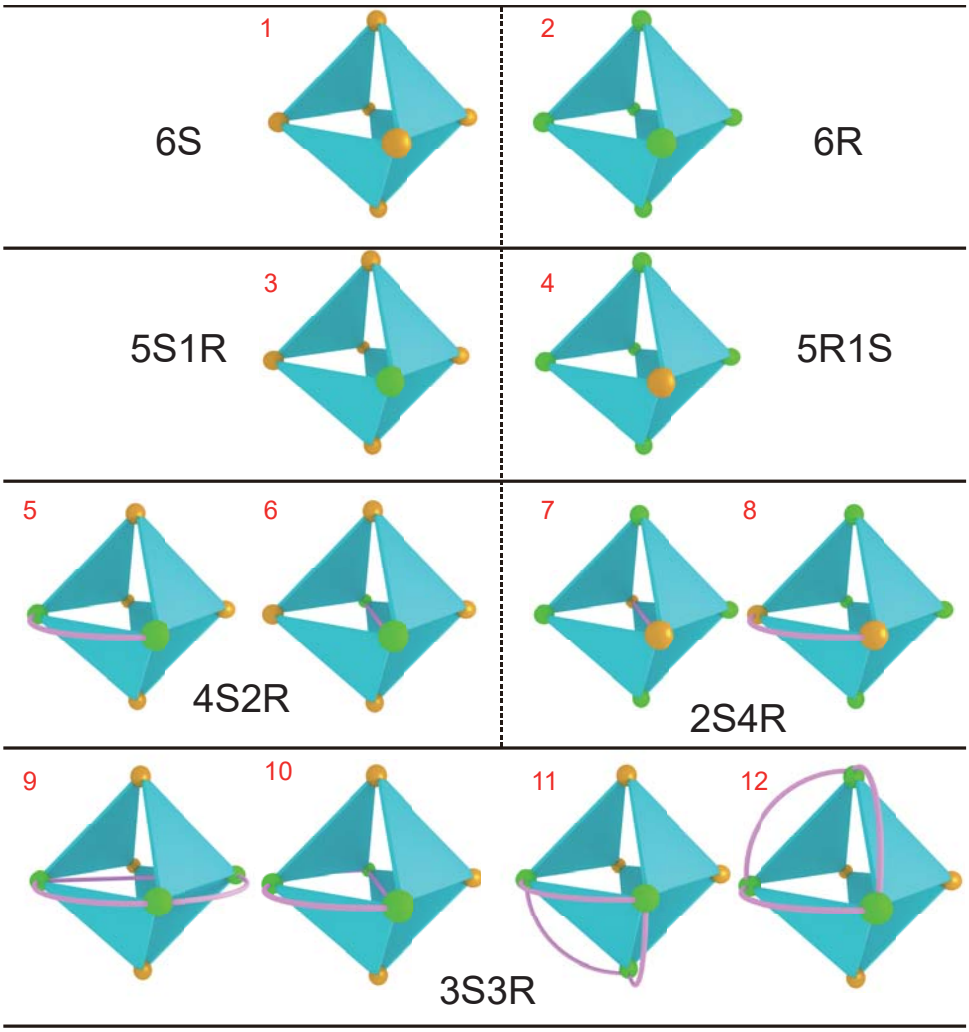

Figure S 27: Permutation of six chiral vertexes in octahedron, yellow and purple balls represent R and S chiral vertices, respectively. Pink sticks were added to better illustrae geometry of polyhedra. When not considering facial directionality, the total number of stereoisomers are 12.

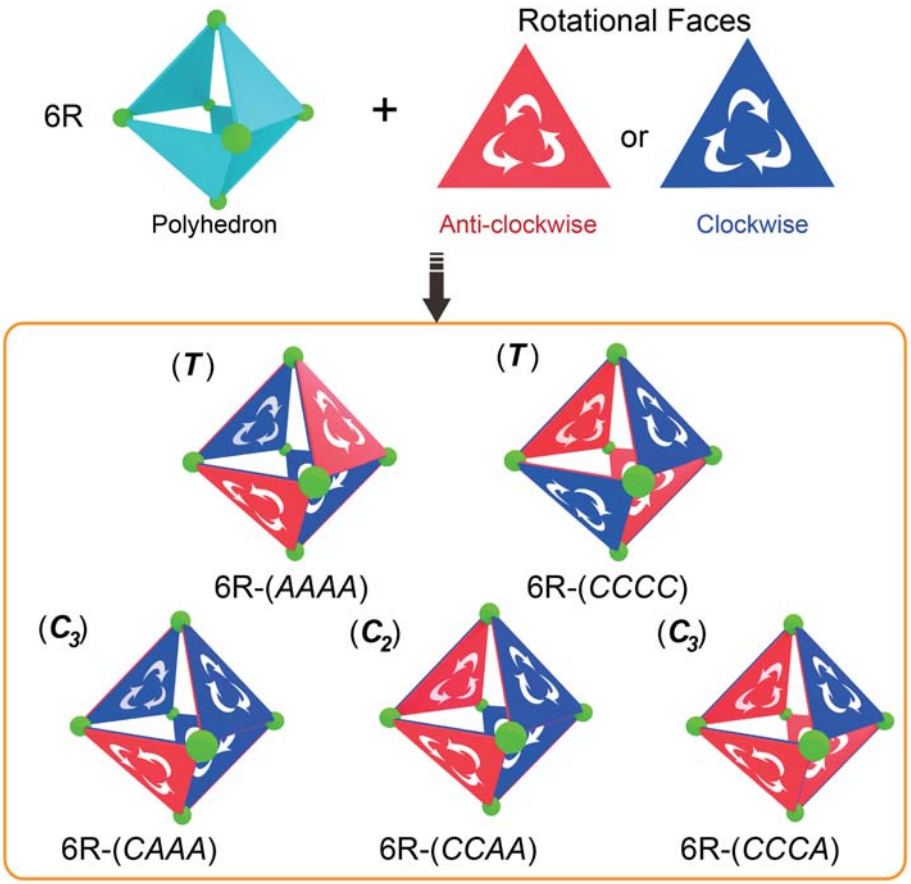

Figure S 28: Five possible stereoisomers of polyhedra **2** composed of six R vertices (6R).

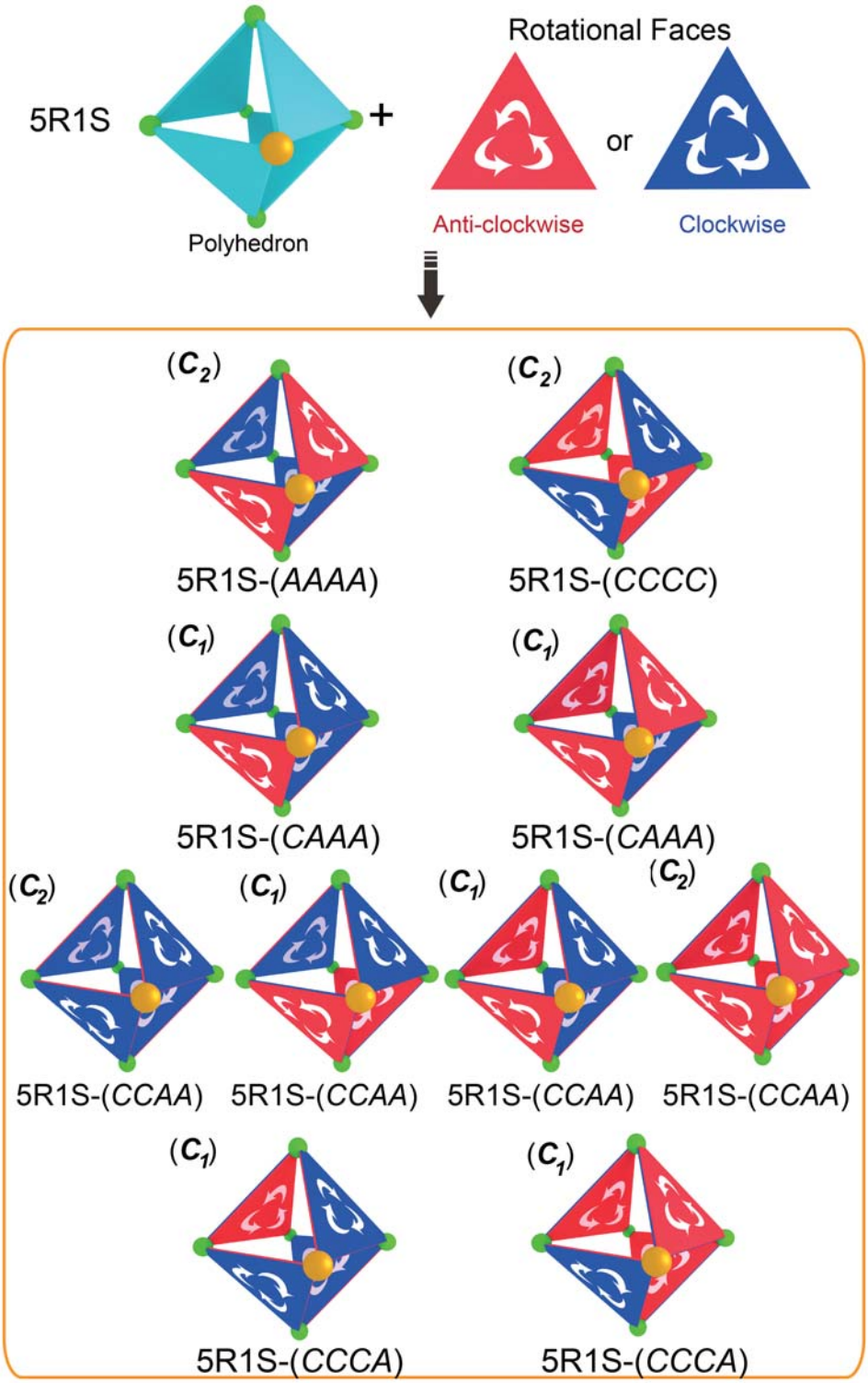

Figure S 29: Nine possible stereoisomers of polyhedra **4** composed of five R-chiral vertices and one S-chiral vertex (5R1S).

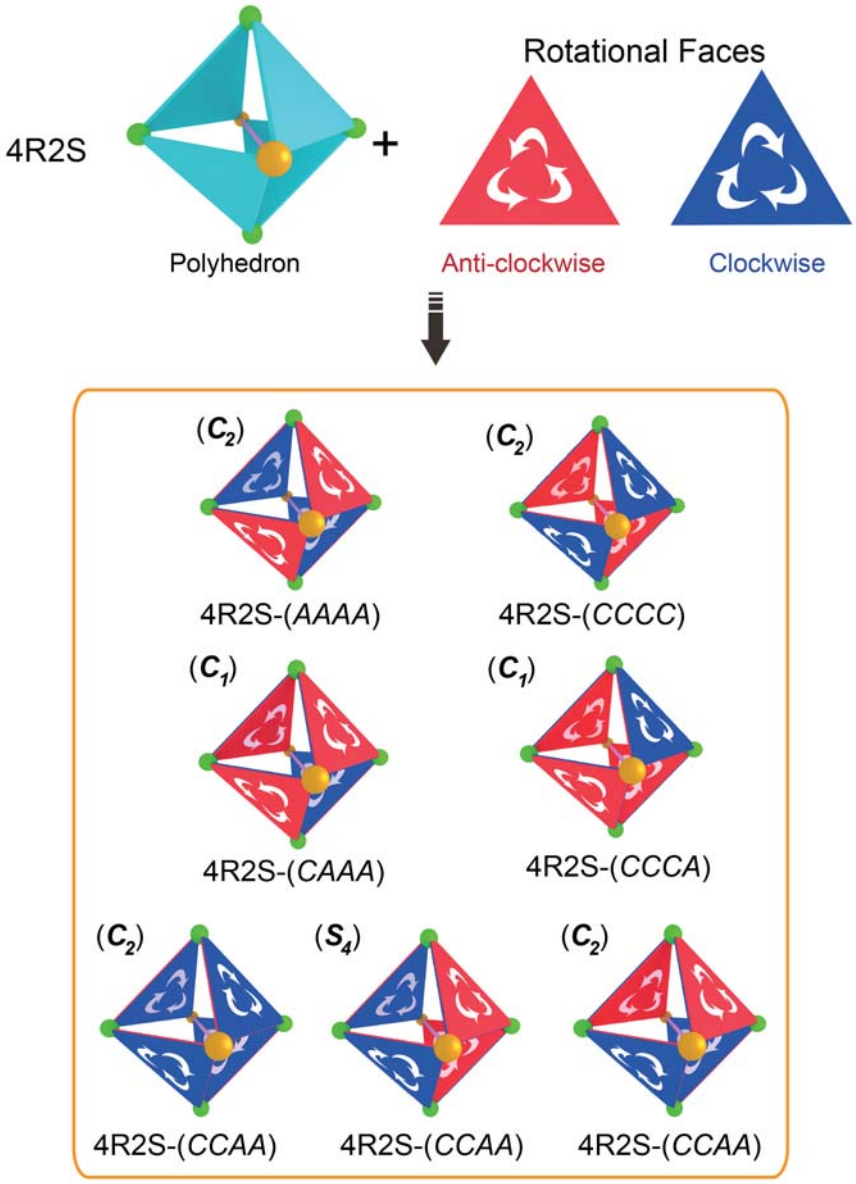

Figure S 30: 7 possible stereoisomers of polyhedron **7**, which is composed of four R-chiral vertices and two S-chiral vertices (4R2S).

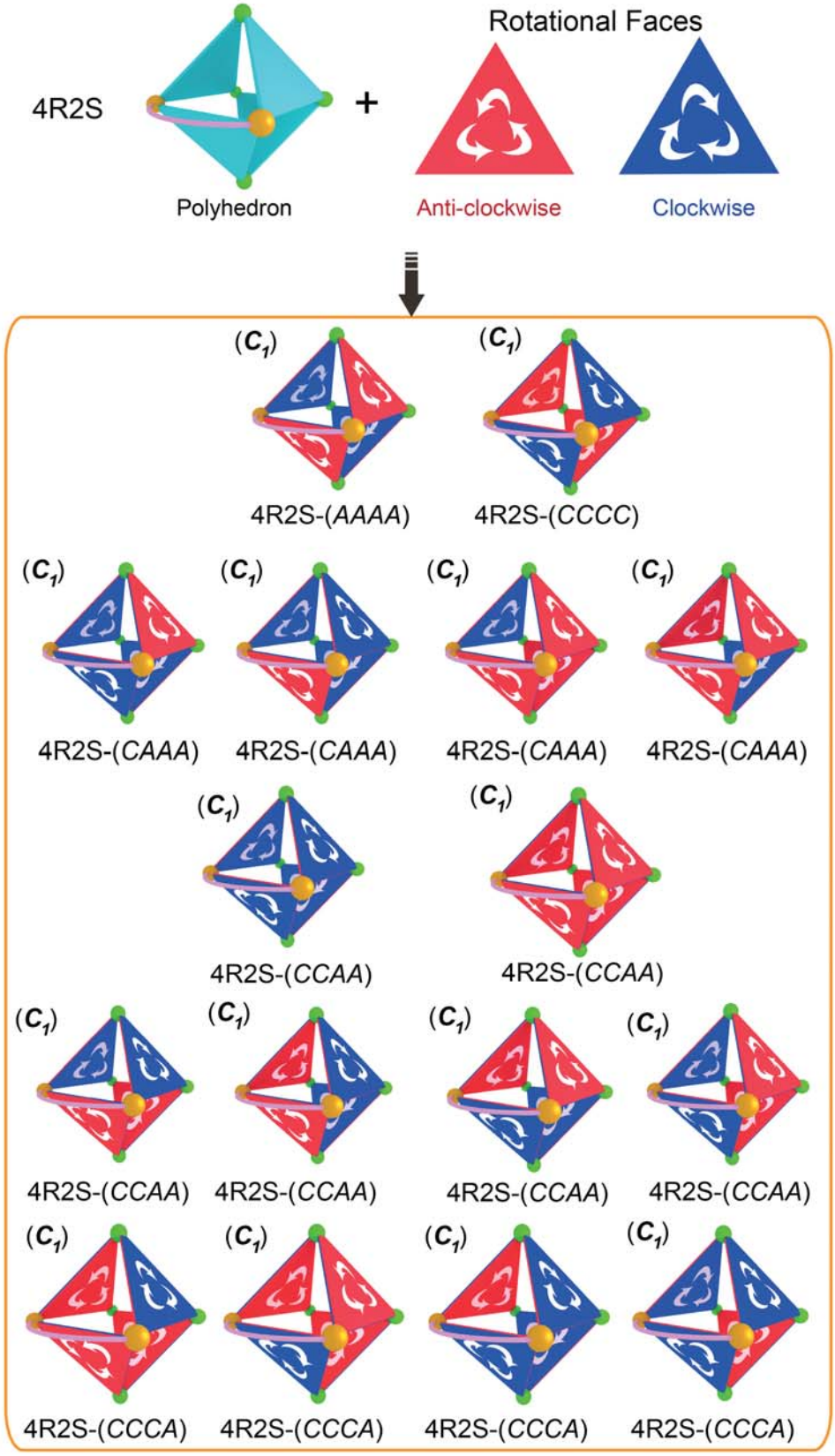

Figure S 31: 16 possible stereoisomers of polyhedron **8** composed of four R-chiral vertices and two S-chiral vertices (4R2S).

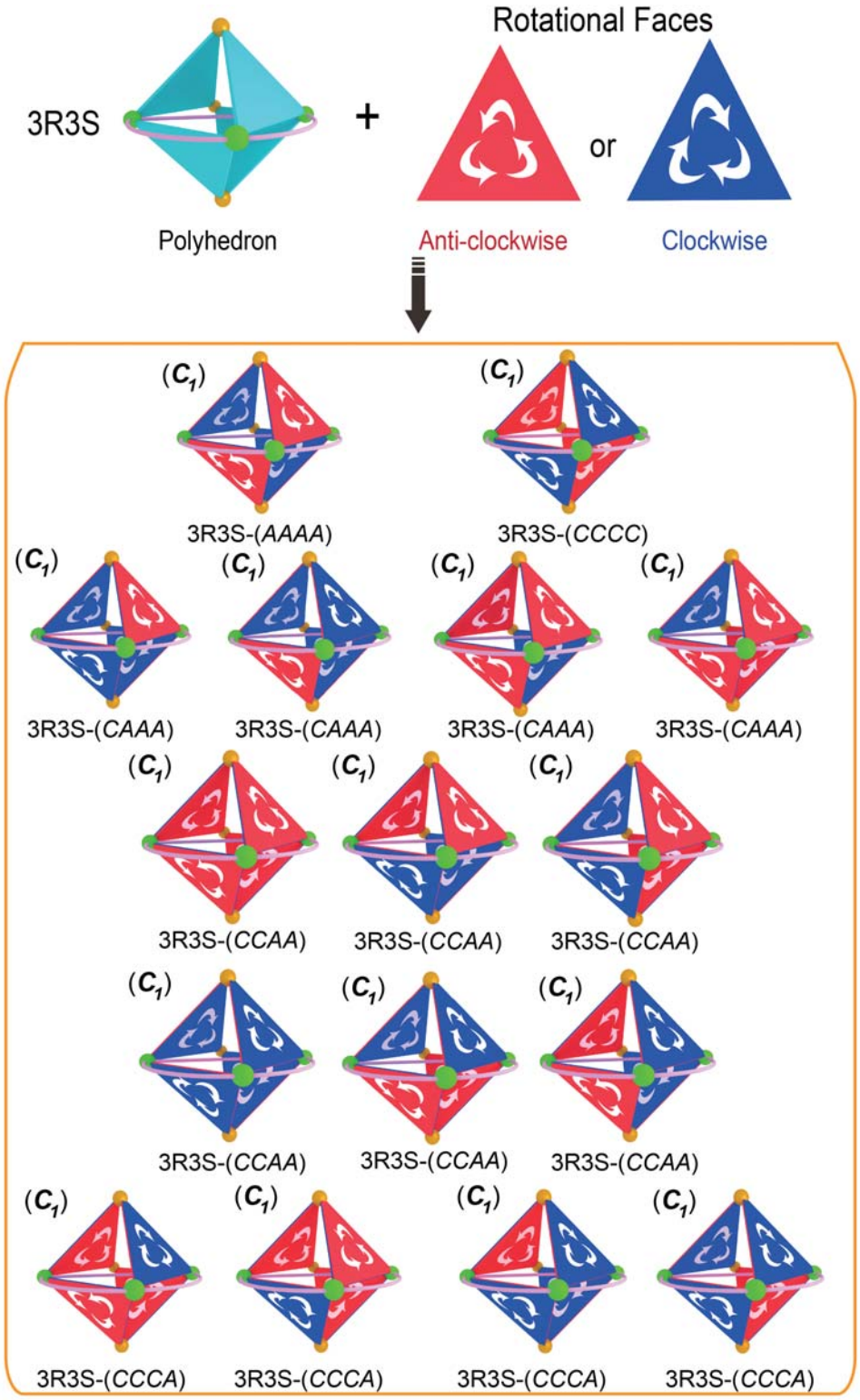

Figure S 32: 16 possible stereoisomers of polyhedra **9** composed of three R-chiral vertices and three S-chiral vertices (3R3S).

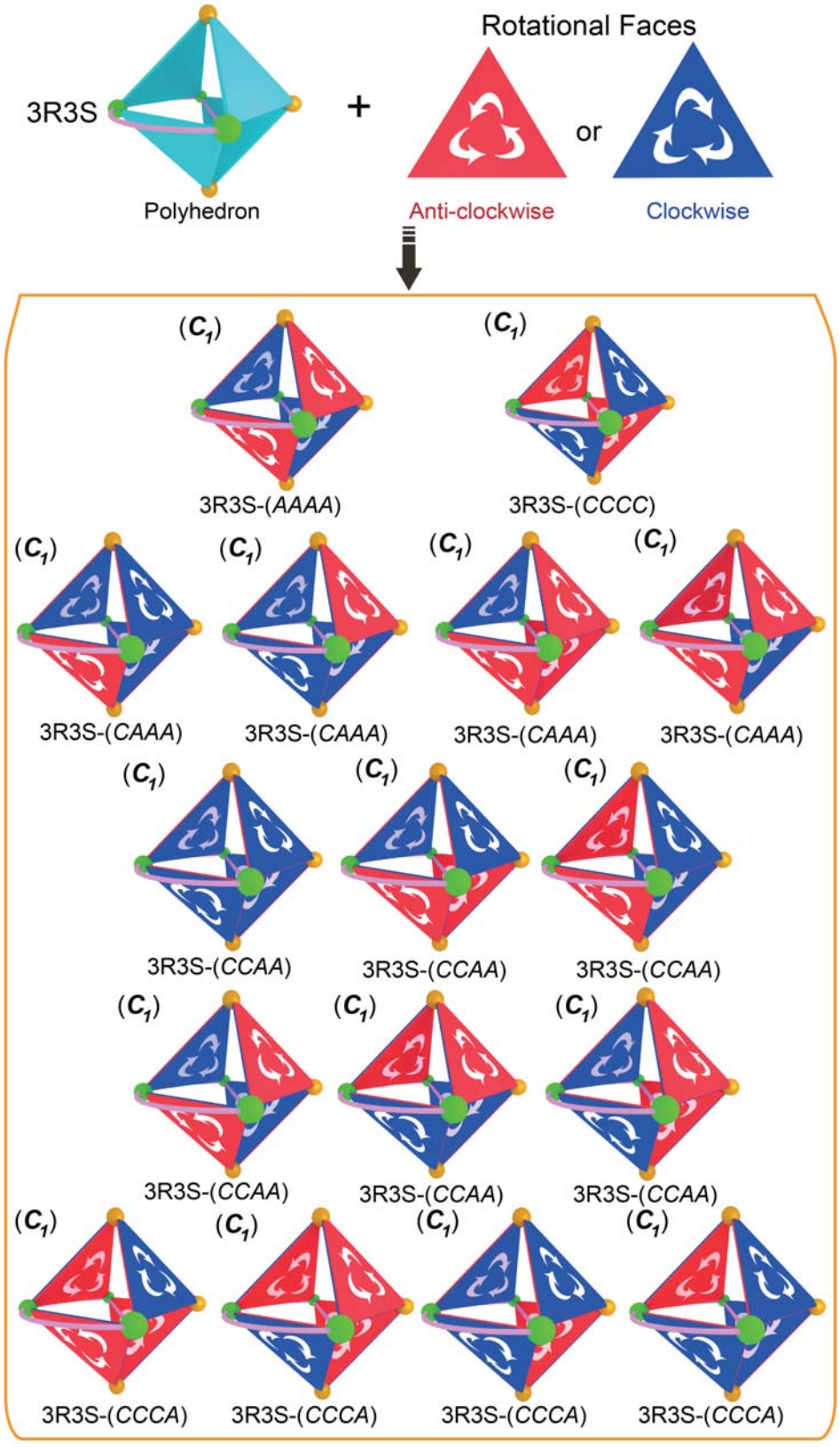

Figure S 33: 16 possible stereoisomers of polyhedra **10** composed of three R-chiral vertices and three S-chiral vertices (3R3S).

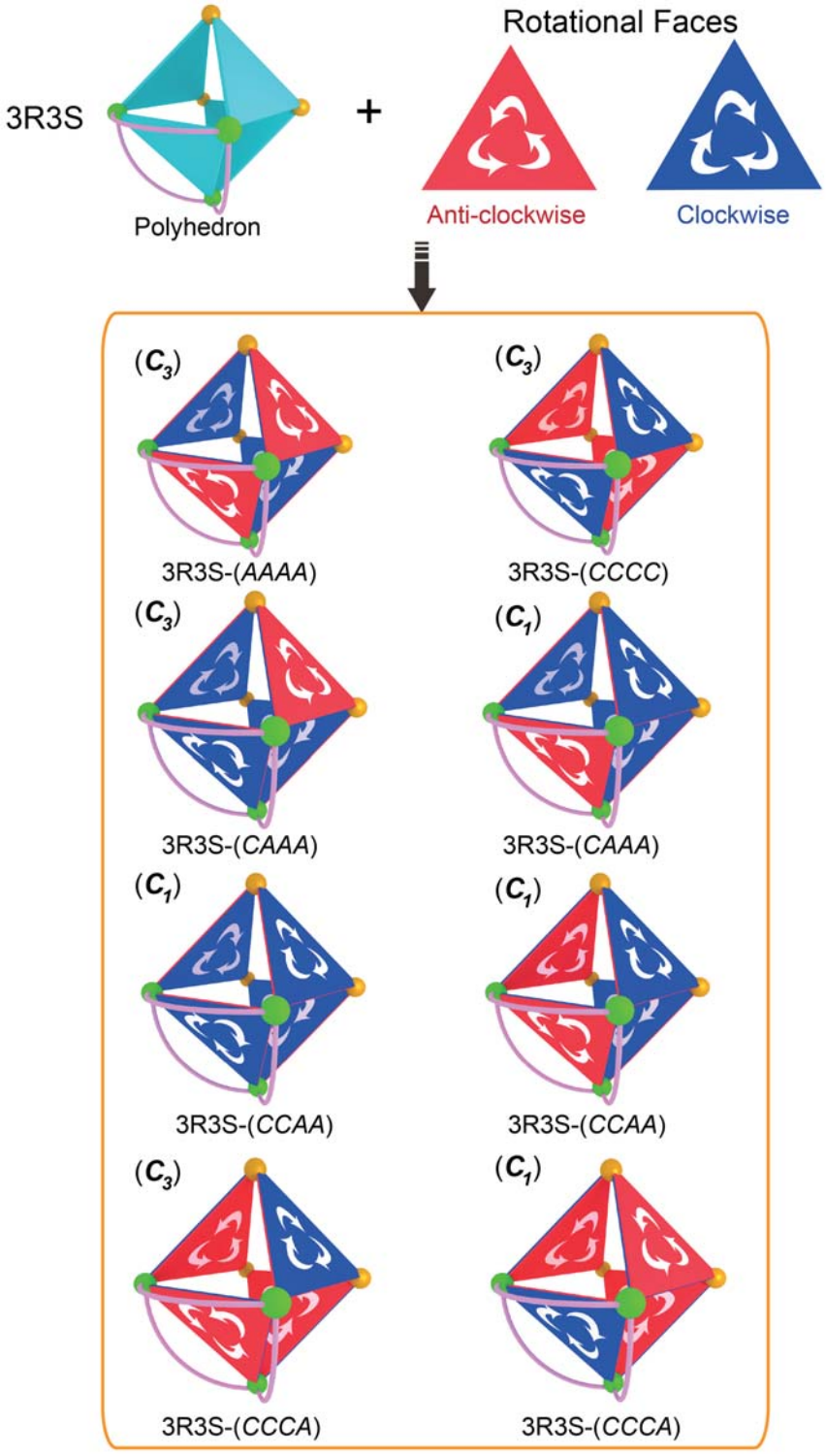

Figure S 34: 8 possible stereoisomers of polyhedra **11** composed of three R-chiral vertices and three S-chiral vertices (3R3S).

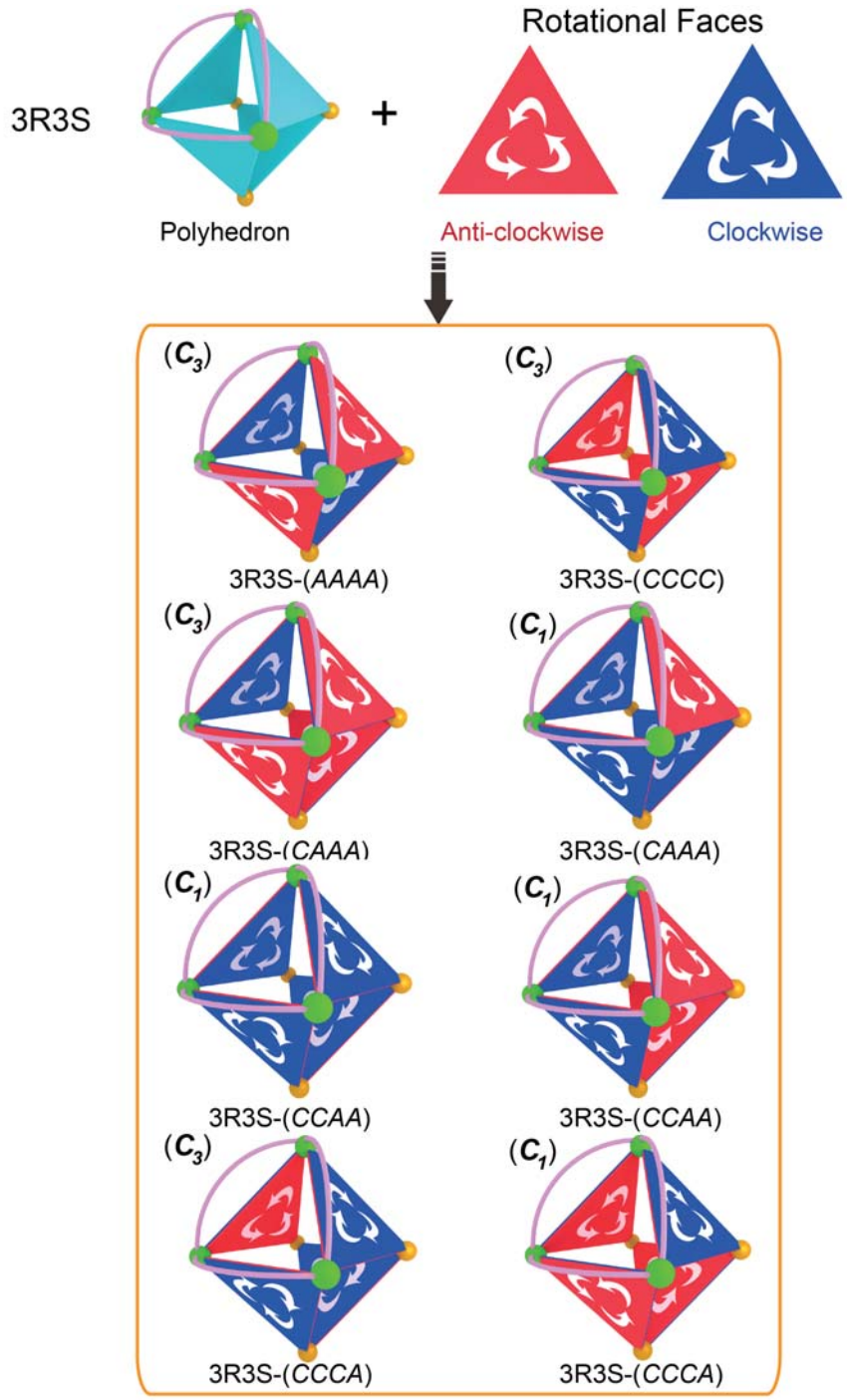

Figure S 35: 8 possible stereoisomers of polyhedra **12** composed of three R-chiral vertices and three S-chiral vertices (3R3S).

6 Crystallography data

6.1 FRP-6

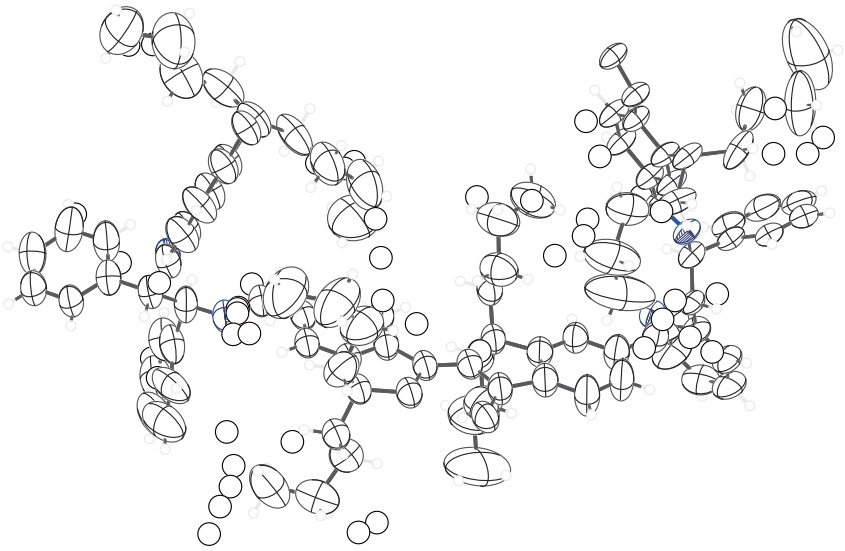

Figure S 36: ORTEP drawing of crystal structures of FRP-**6** (displacement ellipsoids for all non-H atoms at the 50% probability level).

Empirical formula	$C_{300}H_{324}N_{12}$
Formula weight	4097.69
Temperature/K	100.01(10)
Crystal system	trigonal
Space group	R-3
a/Å	24.6800(9)
b/Å	24.6800(9)
c/Å	101.978(5)
α/°	90
β/°	90
γ/°	120
Volume/Å^3	53793(4)
Z	6
ρcalc g/cm^3	0.759
μ/mm^{-1}	0.326
F(000)	13248.0
Crystal size/mm^3	0.5 × 0.5 × 0.5
Radiation	CuKα (λ = 1.54184)
2θ range for data collection/°	7.164 to 131.122
Index ranges	$-28 \leqslant h \leqslant 25$, $-28 \leqslant k \leqslant 28$, $-119 \leqslant l \leqslant 96$
Reflections collected	76208
Independent reflections	20063 [R_{int} = 0.0688, R_{sigma} = 0.0598]
Data/restraints/parameters	20063/189/937
Goodness-of-fit on F^2	1.231
Final R indexes [I$\geqslant$2σ(I)]	R_1 = 0.1260, wR_2 = 0.3615
Final R indexes [all data]	R_1 = 0.1743, wR_2 = 0.4099
Largest diff. peak/hole / e Å^{-3}	0.64/−0.46
CCDC number	1560158

6.2 FRP-7

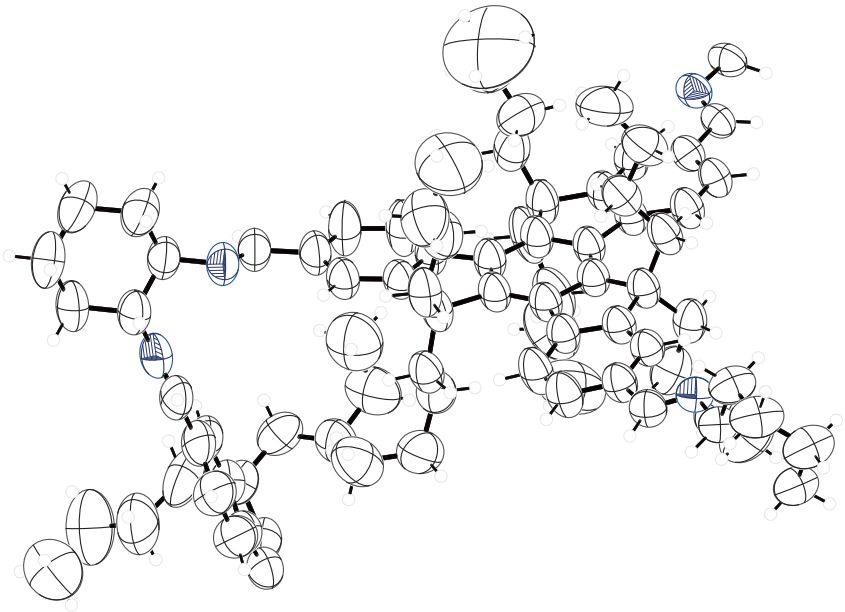

Figure S 37: ORTEP drawing of crystal structures of FRP-**7** (displacement ellipsoids for all non-H atoms at the 50% probability level).

Empirical formula	$C_{252}H_{324}N_{12}$
Formula weight	3521.21
Temperature/K	150.00(10)
Crystal system	trigonal
Space group	P-3
a/Å	27.8827(6)
b/Å	27.8827(6)
c/Å	25.2681(5)
α/°	90
β/°	90
γ/°	120
Volume/Å^3	17012.7(8)
Z	2
ρ_{calc} g/cm^3	0.687
μ/mm^{-1}	0.293
F(000)	3840.0
Crystal size/mm^3	0.3 × 0.2 × 0.2
Radiation	CuKα (λ = 1.54184)
2θ range for data collection/°	6.996 to 147.512
Index ranges	$-33 \leqslant h \leqslant 27$, $-25 \leqslant k \leqslant 34$, $-30 \leqslant l \leqslant 28$
Reflections collected	99624
Independent reflections	22555 [R_{int} = 0.0315, R_{sigma} = 0.0213]
Data/restraints/parameters	22555/0/793
Goodness-of-fit on F^2	1.108
Final R indexes [I$\geqslant$2σ(I)]	R_1 = 0.0971, wR_2 = 0.2951
Final R indexes [all data]	R_1 = 0.1242, wR_2 = 0.3293
Largest diff. peak/hole / e Å^{-3}	0.43/−0.31
CCDC number	1562100

Single-crystal X-ray diffraction

FRP were dissolved in toluene (saturated) and layered with hexane as poor solvent on top. Transparent block crystals were grown within three to seven days. Single crystal X-ray diffraction data were collected on Rigaku SuperNova X-Ray single crystal diffractometer using Cu Kα (λ = 1.54184 Å) micro-focus X-ray sources. Suitable crystal was collected, covered with protective oil and mounted on X-ray diffractometer. The octahedra contain only light elements (*i.e.*, C, H, and N) and the crystal cracks within seconds in air. The crystal was kept in 100 K with liquid nitrogen stream during the unit cell determination and full data collection. The raw data were collected and reduced using CrysAlisPro software, the structures were solved with the SHELXS or SHELXT[1] using Direct Methods and refined with the SHELXL[1] using CGLS minimization, and OLEX2[2] were used as GUI.

Refinement details

All non-hydrogen atoms were refined anisotropically. Hydrogen atoms were placed at calculated positions using the riding model and refined isotropically. The instructions AFIX 23 and AFIX 43 were used for the hydrogen atoms on the secondary -CH_2- and the aromatic C-H, respectively, with the parameter of U_{iso}=1.2 U_{eq}. The instruction AFIX 33 was used for the hydrogen atoms on the highly disordered terminal -CH_3 groups with the parameter of U_{iso}=1.5 U_{eq}. No Shelx restraint was applied to the skeleton of octahedra, *i.e.* truxene faces and diamine vertices. Nevertheless, the flexible butyl groups are expected to be highly disordered, as they are flexible and vibrate randomly in the large voids in the crystal. Therefore, necessary Shelx restraints (i.e., DELU, SIMU, and EADP) were applied to the butyl groups to result a reasonable model. Specifically, the anisotropic displacement parameters of disordered atoms in butyl groups were restrained to be equal within an effective standard deviation of 0.01 using the DELU command. U_{ij} values of disordered atoms of butyl groups were constrained to be similar using the SIMU command. Atomic displacement parameters (ADPs) of different parts of disordered atoms were restrained using the EADP command. There are large voids between the octahedra in crystal, filling with highly disordered solvent molecules. A satisfactory disorder model for the solvent molecules was not found, therefore the OLEX2 Solvent Mask routine (similar to PLATON/SQUEEZE) was used to mask out the disordered density. Crystallographic data have been submitted to the Cambridge Crystallographic Database and are available free of charge.

7 Assembly of TFPT and racemic vertices

7.1 Mass spectra

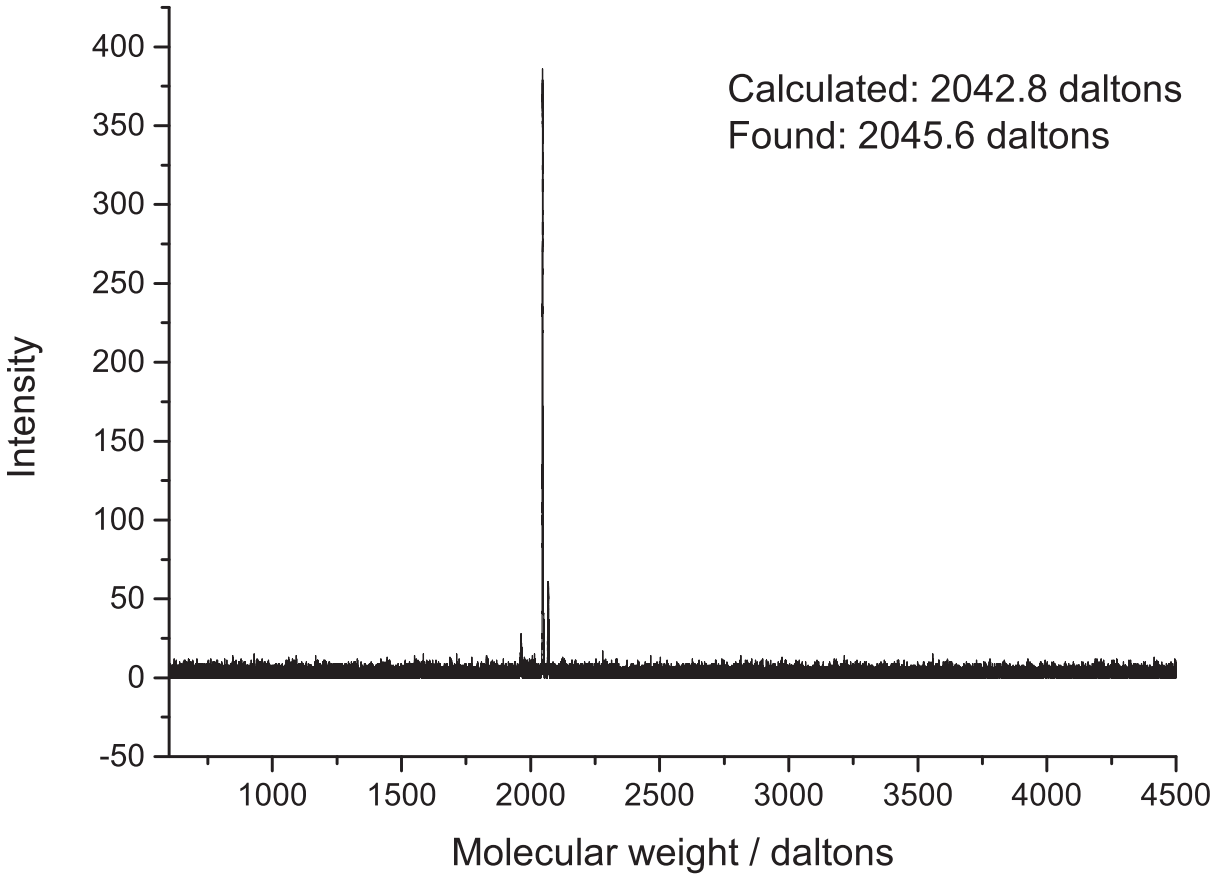

Figure S 38: MAlDL-TOF spectrum of crude products assembled by **TFPT** and *rac*-DPEDA, the peaks found at 2045.6 daltons were calculated to be [4+6] polyhedra.

7.2 NMR spectra

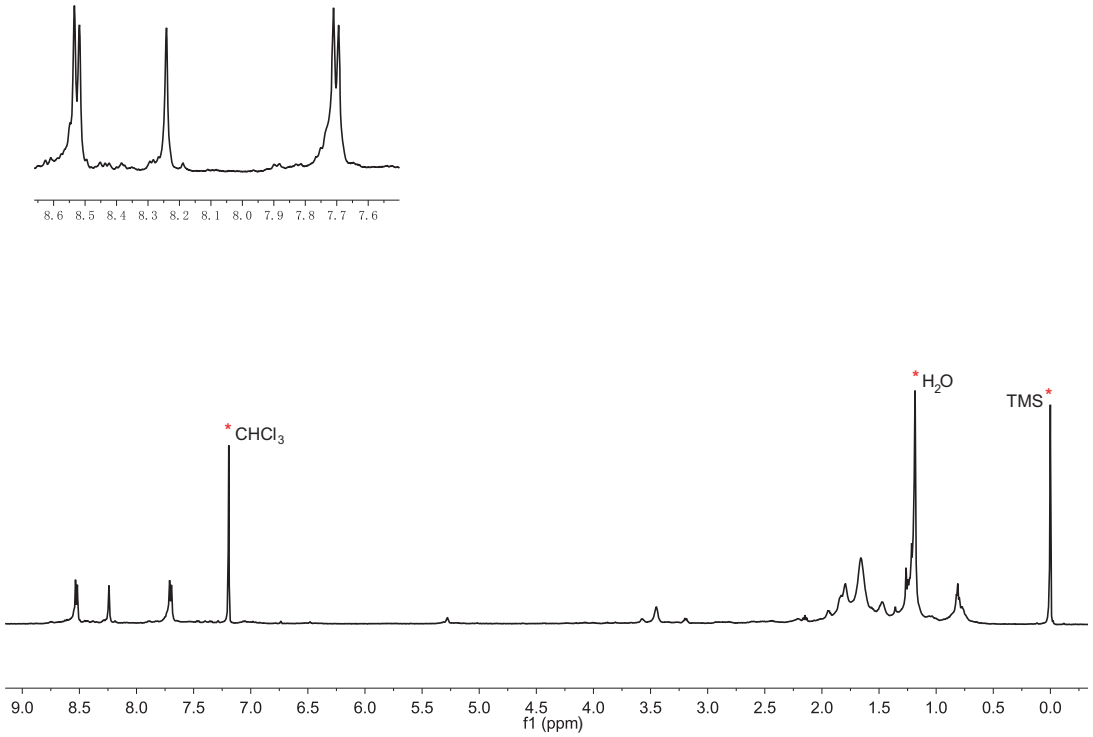

Figure S 39: NMR spectra of crude products assembled by **TFPT** and (1R,2R)-DPEDA without purification.

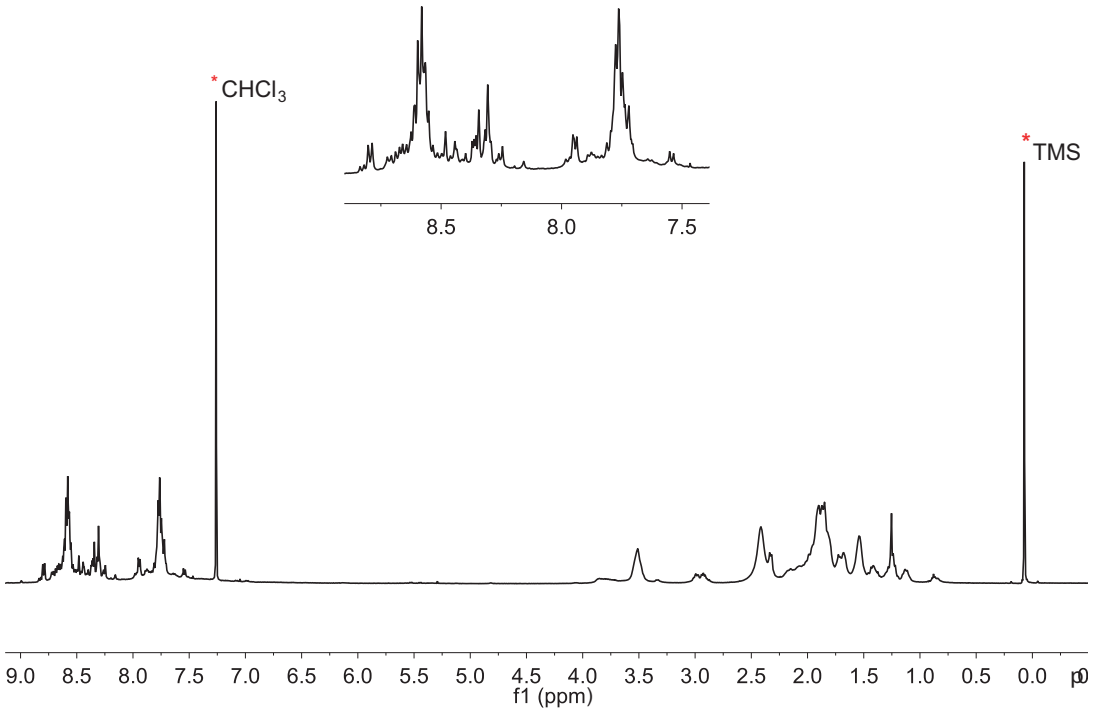

Figure S 40: NMR spectra of crude products assembled by **TFPT** and *rac*-DPEDA without purification.

References:
1. G. M. Sheldrick, A short history of SHELX, *Acta Crystallogr. A*, 2008, **64**, 112-122.
2. Dolomanov, O.V.; Bourhis, L.J.; Gildea, R.J.; Howard, J.A.K.; Puschmann, H., OLEX2: A complete structure solution, refinement and analysis program. *J. Appl. Cryst.*, 2009, **42**, 339-341.